AD/COM

Final Report

Volume II

ADVANCED MEASUREMENT TECHNIQUES FOR COMMUNICATION AND TELEMETRY RECEIVERS

Prepared under

Contract NAS8-21209

Engineering Investigations and Analyses of Communications, Telemetry and Frequency Problems Related to Space Vehicle Systems Instrumentation

May 5, 1969

By

W.H. Lob

S.M. Sussman

J.M. Gutwein

Prepared for

National Aeronautics & Space Administration
Marshall Space Flight Center
Huntsville, Alabama 35812

by

ADCOM
A Teledyne Company
808 Memorial Drive
Cambridge, Massachusetts 02139

G-99F

TABLE OF CONTENTS

TABLE OF CONTENTS (Cont)

LIST OF ILLUSTRATIONS

LIST OF ILLUSTRATIONS (Cont)

1. INTRODUCTION

A review of specifications of commercially available receivers reveals a myriad of parameters pertinent to performance capabilities, with each manufacturer emphasizing certain claims and design features of his equipment. Unfortunately standardized measurement procedures do not exist for measuring the various performance characteristics of receivers. Consequently, a user experiences difficulty in verifying performance claims of certain receivers or in comparing the quoted performance specifications of commercially available units.

The purpose of this document is to describe experimental procedures which best measure and characterize important performance properties of communication and telemetry receivers. The procedures described are in general, applicable to any receiver, however, the discussions are presented in the context of FM telemetry receivers and digital PCM equipment. The procedures outlined do not purport to cover all receiver specifications; rather, those specifications which bear upon the interference rejection capabilities of receivers are given priority along with those for which a certain amount of uncertainty or controversy persists.

Sections 2 through 5 of this report deal specifically with receiver measurement procedures. Sections 6 and 7 cover measurements pertinent to PCM telemetry receivers and interface equipment. The receiver measurements sections concentrate on performance characteristics relating to receiver sensitivity, dynamic range, non-linear spurious responses, IF filter properties such as group delay and noise bandwidth, AGC response times and receiver capture performance. In addition, techniques are described for conducting telemetry baseband noise loading measurements in order to identify various receiver-transmitter distortion producing mechanisms.

The sections dealing with digital PCM telemetry equipment outline procedures for measuring synchronization parameters such as PCM clock phase error and bit error rate. Procedures are discussed for measuring PCM frame sync loss. Finally, tests are suggested for measuring these PCM performance characteristics under the handicap of an inaccessible transmitter.

2. FRONT-END TESTS

The front end (RF pre-selector, amplifier, and mixer) should be tested for three performance parameters:

1. Noise figure
2. Selectivity, in particular the rejection ratio for the image and other linear spurious responses
3. Intermodulation products and other non-linear spurious responses.

In these tests the IF amplifier and FM detector will be used as part of the test equipment. Their performance, however, should not materially affect the test results.

2.1 Noise Figure Measurement

2.1.1 Discussion

The optimum noise figure F_o of an amplifier is defined[1] as the ratio of the noise spectral power density* (N_{ao}) available in the amplifier output to that part (N_{aos}) of this output which is due solely to a noise-matched source at standard temperature at the input to the amplifier. Alternatively, it is the available input SNR in a given frequency band divided by the corresponding SNR in the amplifier output. Using the first of these definitions, we have

$$F_o \equiv N_{ao}/N_{aos} = [\overline{E_o^2}/(R_o B_N)]/(N_{as} G_a) , \qquad (1)$$

where

$\overline{E_o^2}$ = the mean square noise output voltage of the amplifier

R_o = the resistive part of the amplifier output impedance

B_N = the noise bandwidth of the amplifier

N_{as} = the available input noise spectral power density of the source at 290°K

G_a = the available power gain of the amplifier.

---

*Spectral power density N(f), also called noise density, power per unit bandwidth, or incremental power, is here defined such that $\int_0^\infty N(f)df = P$, the total power.

The input available noise power density, N_{as}, is given by

$$N_{as} = k T_o, \tag{2}$$

where

$k = 1.374 \times 10^{-23}$ joules/^oK (Boltzmann's constant)

T_o = the standard reference temperature of 290^oK.

Also[2]

$$G_a = (R_s/R_o)\left|H(f)Z_i/(Z_i + Z_s)\right|^2, \tag{3}$$

where

$Z_s = R_s + jX_s$ = the source impedance

R_o = the resistive part of the amplifier output impedance

$|H(f)|$ = the amplifier's frequency response

Z_i = the amplifier's input impedance.

Substitution of (2) and (3) in (1) yields

$$F_o = \frac{\overline{E_o^2}}{kT_o A^2 B_n R_s} \left| \frac{Z_i + Z_s}{Z_i} \right|^2, \tag{4}$$

where use of the noise bandwidth justifies replacement of $|H(f)|$ by $A \equiv |H(f_o)|$, the amplifier's voltage gain at the center frequency f_o.

2.1.2 Procedure

Note: This test requires either accessibility of the IF amplifier's output port or use of an auxiliary amplifier with known noise bandwidth. In the latter case the mixer output must be accessible.

1. Tune the receiver to a completely empty channel. (If such a channel does not exist, a less realistic test using a dummy antenna will have to be run. In that case the receiver tuning is immaterial.)

2. Replace the antenna by an unmodulated RF signal generator tuned to the center frequency of the channel.

3. With the AGC line (if any) disabled, adjust the amplitude of the test signal so that it is well above the front-end noise yet does not overdrive the last IF amplifier stage. This may require connecting the AGC line (if any) to a dc voltage to reduce the IF gain, or reducing the IF gain in some other way. If this condition cannot be achieved, an auxiliary tuned amplifier with a comparable pass band, known noise bandwidth, and less gain will have to be used instead of the receiver's IF amplifier.

4. Observe the test signal at the IF (or auxiliary) amplifier output and determine the voltage gain A from the receiver input terminals to the IF (or auxiliary) amplifier output. Make sure amplifier is operating linearly.

5. Disconnect the signal generator and reconnect the antenna (the dummy antenna if there is no empty channel).

6. Measure the rms noise V_{rms} at the IF (or auxiliary) amplifier output. (Ensure that there is no limiting of the noise by the last stage.)

7. The optimum noise figure F_o can now be calculated from the relation

$$F_o = \frac{V_{rms}^2}{kT_o A^2 B_n R_a} \left| \frac{Z_i + Z_a}{Z_i} \right|^2, \tag{5}$$

where

$k = 1.374 \times 10^{-23}$ (Boltzmann's constant)

$T_o = 290^{\circ}K$

A = the previously measured voltage gain

B_n = the IF- (or auxiliary) amplifier noise bandwidth in Hz (see Sec.)

$Z_a = R_a + jX_a$ = the antenna impedance

Z_i = the receiver input impedance

Note that if at the frequencies of interest the antenna is well matched to the receiver and looks mostly resistive, (5) simplifies to

$$F_o = \frac{V_{rms}^2}{4KT_o A^2 B_n R_a}. \tag{6}$$

2.2 Tests for Spurious Responses

2.2.1 Discussion

The image response of a superheterodyne receiver is a linear phenomenon caused by imperfect rejection by the RF preselector of a frequency $2f_i$ removed from the center frequency of the tuned receiver, where f_i is the intermediate frequency. Another source of linear spurious responses can be the harmonic content of the local oscillator output. This will give rise to responses at $nf_{lo} \pm f_i$, $n=2,3,\ldots$, where f_{lo} is the local-oscillator frequency.

If the active elements in the front end are driven into their non-linear region, additional spurious responses arise due to the possibility of harmonics and intermodulation products falling into the pass band.

The two tests to be described will show the degradation due to both linear and non-linear spurious responses.

2.2.2 The Front End RF Noise-Loading Test

2.2.2.1 Discussion

In the first of these tests, the RF environment of the receiver will be simulated by broad-band RF noise, from which the RF equivalent of the IF pass band can be removed by a band-rejection filter. Thus when the filter is in use, the only noise reaching the FM detector is that due to spurious responses, whereas when the filter is bypassed, almost all of this noise is due to the desired receiver response. In this way a desired-to-spurious response ratio can be determined. This ratio will be independent of the noise density of the input noise as long as the receiver front end is operating linearly, and will decrease with increasing input noise density once higher-order spurious responses come into play (Fig. 1). Thus one may set a lower limit on the allowable desired-to-spurious response ratio, and use the corresponding input noise density as a measure of the upper end of the receiver's dynamic range. This may be compared against the front-end noise density N_f, obtainable from the optimum noise factor by

$$N_f = kT_o(F_o - 1) \approx 4 \times 10^{-21}(F_o - 1) . \qquad (7)$$

Because of the likelihood of overdriving the last stage(s) of the IF amplifier in this test, the "noise reaching the FM detector" is best measured indirectly by the noise quieting method. In this method, an unmodulated carrier at the RF center frequency is introduced into the receiver front end in

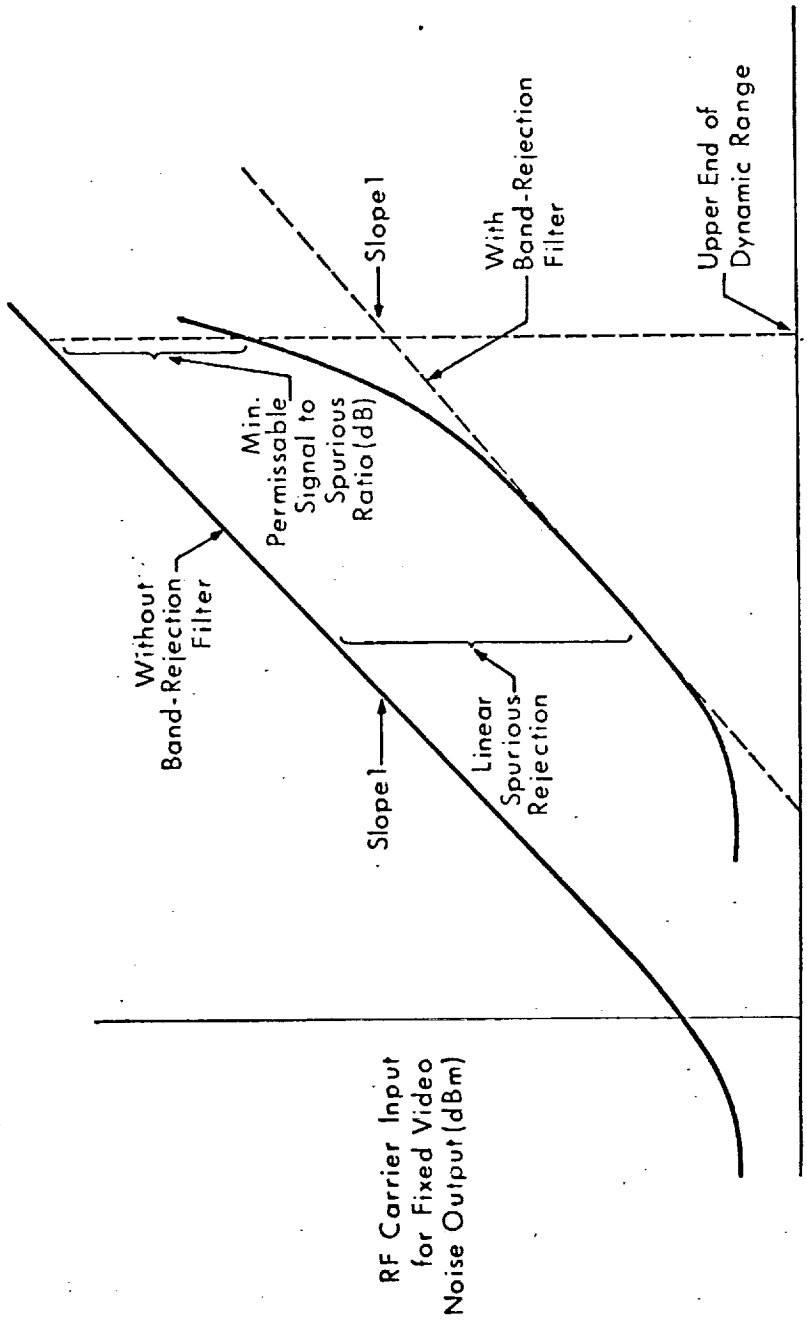

Fig. 1 Spurious Response Test Results

addition to the broadband noise. Throughout the test the level of this carrier is adjusted to yield a fixed level of video noise in the FM detector output. Since the noise output from an FM detector depends only on the carrier-to-noise ratio at its input, this power level of the RF carrier is a direct measure of the power of the noise co-existing with the carrier at whatever point in the circuit limiting first takes place.

2.2.2.2 Equipment (see Fig. 2)

The broad-band noise source should generate noise whose spectral power density is essentially flat from the receiver's intermediate frequency f_i to $4f_{lo} + f_i$, where f_{lo} is the local oscillator frequency. Commercial noise sources, covering all the RF bands of interest are manufactured by: Hewlett Packard, Palo Alto, Calif.; Airborne Instruments Laboratory, Deer Park, L.I., N.Y.; General Microwave, L.I., N.Y.; and others.

Broad-band amplifiers are available from Avantek, Santa Clara, Calif.; C-Cor, State College, Penn.; and others.

Suggested specifications for the band rejection filter are as follows:

1) Over the RF-equivalent of the 3dB IF passband, the filter's relative* attenuation should exceed the best image rejection ratio likely to be encountered in the receivers to be tested. In view of the receiver specifications commonly encountered, 60 dB relative attenuation would seem to be adequate, 80 dB would seem ample.

2) The filter should have a 60dB/6dB shape factor of 6 or less. Clearly, a separate filter needs to be provided for each tuner setting to be tested.

The filter may have to be realized in several sections, separated by amplifiers for isolation and gain. In that case the last unit in the cascade should be a filter section in order to remove any distortion products generated in the last amplifier.

Filters of this kind are manufactured to specifications by Vector Industries, Palo Alto, Calif.; I-Tel, Kensington, Md.; Microwave Development Laboratories, Needham, Mass.

---

* Relative attenuation: The attenuation in the rejection band compared to that in the pass band.

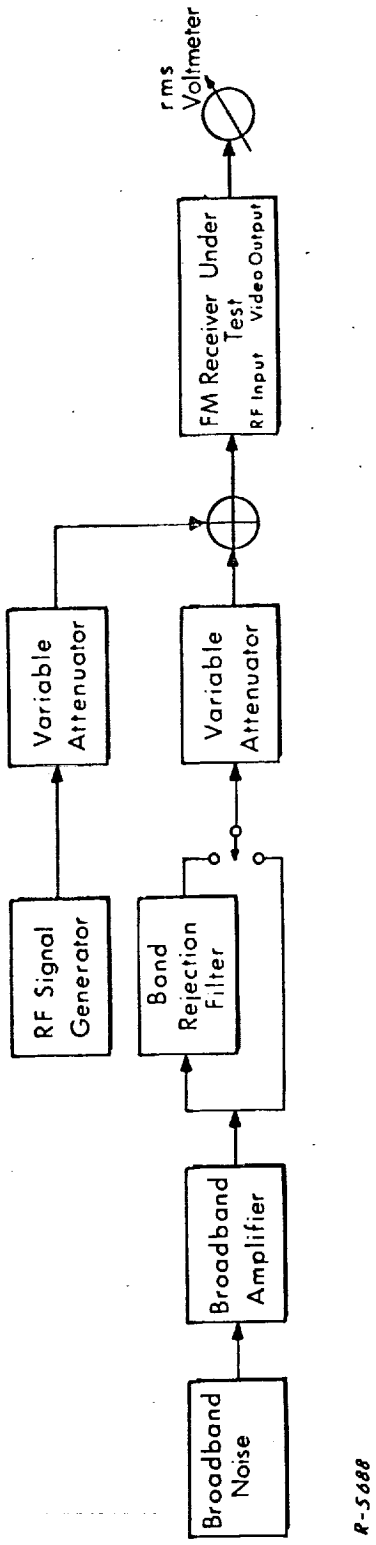

Fig. 2 Setup for Spurious Response Test using Noise Loading

2.2.2.3 Procedure (see Fig. 2)

1. Switch the band-rejection filter out of the circuit.
2. Determine the "signal only" and "noise only" readings of the RMS voltmeter. Clearly, when obtaining the "signal only" reading, the signal must be strong enough to saturate the FM detector, as evidenced by the fact that a further increase of input signal does not materially affect the meter reading. Similarly, for the "noise only" reading, the voltmeter indication should be unaffected by a further increase in input noise.
3. Choose a convenient value for the "given" RMS voltmeter reading to be maintained for the balance of this test, except that this value should be greater than three times the "signal only" reading (or 10dB higher) and less than one third of the "noise only" reading (10dB less).
4. Vary and record the noise input together with the signal input required to obtain the "given" RMS voltmeter reading.
5. Repeat step 4 with the band-rejection filter in the circuit, using the same value for the given reading as in step 4.

2.2.3 The Weak-signal, Strong-interference Test

2.2.3.1 Discussion

A further test on spurious responses due to limited front-end selectivity and linearity is the weak-signal, strong-interference test. It has the advantage over the previously described noise-loading test of pinpointing some of the spurious response frequencies for a particular receiver at a particular tuning. More specifically, it will reveal the spurious responses due to a single interfering signal, such as the image response and the fractional-IF responses. On the other hand, it will not indicate responses due to third-order intermodulation products of two simultaneous out-of-band interfering signals.

The test requires a weak "desired" FM carrier, whose center frequency is the nominal RF frequency which the receiver is tuned to, and whose sinusoidal, high-index modulation sweeps out the IF bandwidth quasi-statically. The interfering signal is basically unmodulated, except that its frequency should be variable through the entire RF spectrum at a rate much less than the peak sweep rate of the "desired" signal of interest.

The quantity to be observed is the fundamental modulation component in the video output of the receiver. The fact that this component will be present or absent, depending on whether, at the limiter input, the desired signal is stronger or weaker, respectively, than the interfering frequency component, is the basis for this test.

By simultaneously varying the levels of both input signals in such a way as to keep a particular spurious "dropout" on the verge of disappearing, we can determine whether the offending interfering frequency component varies proportionately with, or as some higher power of, the interfering input signal level, hence whether the spurious response is due to inadequate selectivity or to having surpassed the upper end of the dynamic range.

2.2.3.2 Procedure (Fig. 3)

1. With the interfering-signal generator turned off, bring up the amplitude of the desired signal until the modulation appears reasonably clean on the scope (this adjustment is not critical).
2. Sweep the interfering signal frequency from f_i to $4f_{lo} + f_i$ (f_i = intermediate frequency; f_{lo} = local oscillator frequency) while slowly increasing its amplitude until one or more spurious "dropouts" of the modulation output appear.
3. Investigate each of the observed spurious responses for linearity. To this end keep the interfering signal frequency fixed and simultaneously increase the amplitudes of both input signals so as to keep the fundamental modulation output at the verge of appearing. Check the corresponding levels of the input signals to see whether the amplitude of the desired input signal had to be increased in proportion to, or faster than, the amplitude of the interfering input signal.

If any of the spurious dropouts thus investigated exhibits higher-order behavior, the upper end of the dynamic range has been exceeded. If not, resume step 2 at a higher level of the interfering input signal until new spurious dropouts appear. Then investigate these for linearity, etc.

The dynamic range can be taken as the ratio of the power level of the lowest level out-of-band interfering signal (regardless of where it is located in frequency) which produces a non-linear spurious response to the power level of a desired signal causing threshold operation of the receiver (see Sec. 2.1).

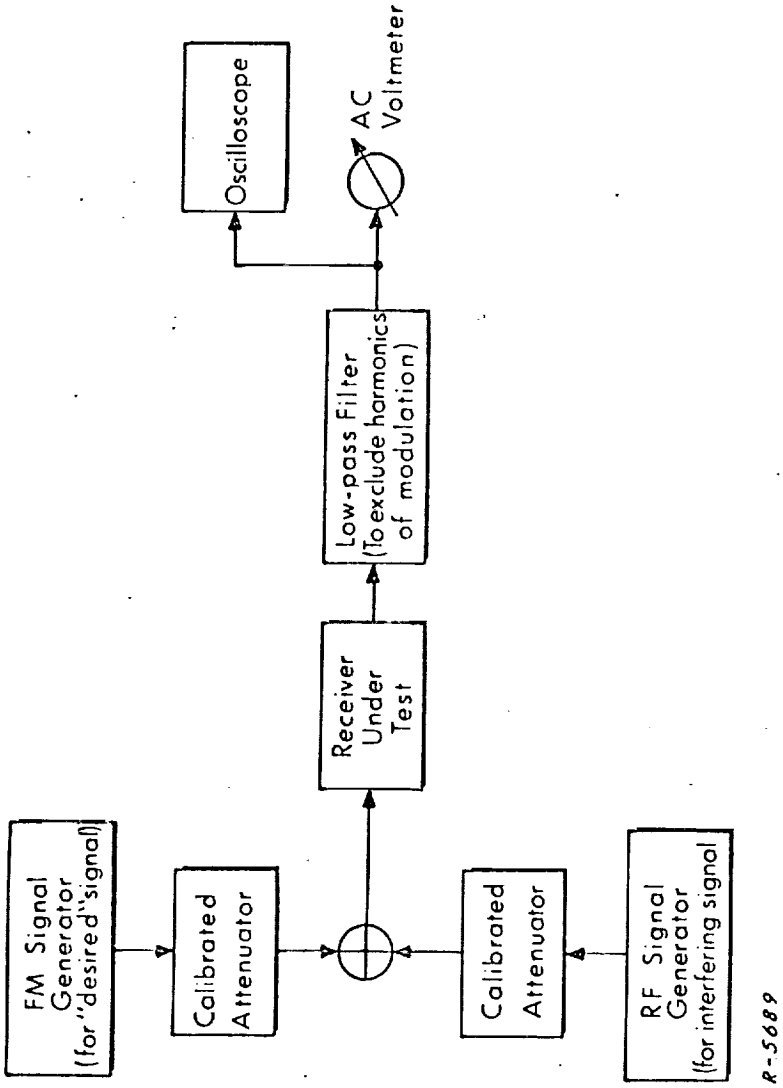

Fig. 3 Setup for the Weak-signal, Strong-interference Test

3. IF AMPLIFIER TESTS

The following tests for the IF amplifier are of primary interest:

1. Frequency response measurement
2. Group delay measurement
3. Noise bandwidth measurement

These three tests require that the IF amplifier's input and output ports are accessible.

3.1 Frequency Response Measurement

This test is best performed with a commercial swept-frequency signal generator and an oscilloscope, as shown in Fig. 4. The following precautions should be observed.

1. In receivers with AGC, the AGC line should be disconnected from the AGC detector and connected to an adjustable dc voltage. The IF frequency response should be obtained for various values of this dc voltage to check for a possible dependence of the shape of the response upon the AGC voltage.
2. The test signal should be attenuated sufficiently to prevent the IF amplifier from being overdriven. This can be verified by
   a) stopping the sweep action of the signal generator, and with the now unmodulated signal held in the pass band of the amplifier, checking the waveform of the IF output, or
   b) generating the frequency response display at two different input signal levels. If the responses are of identical shape, the amplifier is operating linearly.
3. The sweep rate should be as low as possible in order to obtain good spectral resolution. If a further lowering of the sweep rate does not noticeably alter the observed response, the sweep rate is sufficiently low.

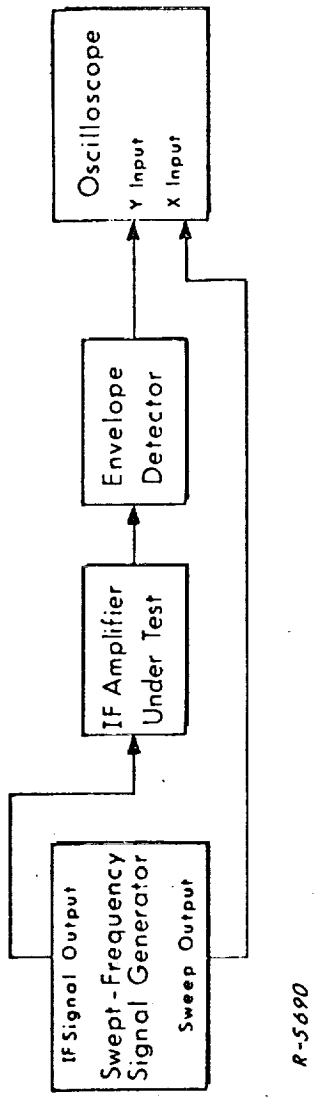

Fig. 4 Frequency Response Measurement of IF Amplifier

3.2 Group Delay Measurement

It has been pointed out[4] that in FDM/FM systems the control of the group delay of the IF amplifier is more important than that of amplitude ripple in the frequency response. The group delay is usually measured by amplitude modulating a carrier and observing the variation of delay of the envelope as the carrier frequency is changed through the band of interest. Equipments for generating and analyzing the required signals are manufactured by Acton Laboratories, Acton, Mass.; Sierra Electronics Operation of Philco-Ford, Menlo Park, Calif.; Wandel & Goltermann, Reutlingen/Germany; Wiltron Co., Palo Alto, Calif.; and others.

The same precautions apply to this test as to the measurement of the IF amplifier frequency response.

3.3 Noise Bandwidth Measurement

The noise bandwidth is defined by the relation

$$B_N \equiv \int_0^\infty |H(f)|^2 \, df / |H(f_o)|^2, \tag{8}$$

where f_o is the center frequency of the amplifier, so that $|H(f_o)|$ is the gain of the amplifier (in factor). Most IF amplifiers, when properly aligned, have sufficiently sharp cutoff characteristics to make the noise bandwidth very nearly equal to the 3 dB bandwidth.

The noise bandwidth may be calculated[3] from the measured frequency response of the IF amplifier using Eq. (8). Alternatively, a direct measurement of the numerator of (8) is possible with a noise source whose power density is known to be constant over the spectral region of interest. If the output of such a source of spectral density N_o is applied to the input of the amplifier under test, the mean square value of the amplifier output is given by

$$\overline{E_o^2} = N_o \int_0^\infty |H(f)|^2 \, df. \tag{9}$$

Thus a measurement of $\overline{E_o^2}$ will yield a value for the integral if N_o is known. If N_o is not known, the noise source may be calibrated by applying its output to a series LRC circuit tuned to f_o as shown in Fig. 5.

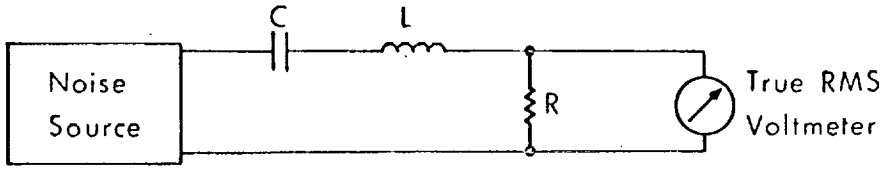

Fig. 5 Measurement of the Noise Source Spectral Density

The noise bandwidth of this circuit is

$$b_N = (R + r)/4L, \tag{10}$$

where r is the resistance of the inductor $(2\pi fL/Q)$, and the power delay of the source is given by

$$N_o = 4\overline{E_m^2}L(R + r)/R^2, \tag{11}$$

where $\overline{E_m^2}$ is the square of the RMS voltmeter reading.

By combining (8), (9) and (11) we find

$$B_N = \frac{\overline{E_o^2}}{\overline{E_m^2}} \cdot \frac{R^2}{4(R + 4)L\left|H(f_o)\right|^2}. \tag{12}$$

3.4 AGC Measurements

The performance of the AGC circuitry (if any) may be tested for tracking and response times. Both tests require access to the IF amplifier output.

3.4.1 AGC Tracking Measurement

By AGC tracking is meant the degree by which a quasi-static change in signal level is reduced in the IF amplifier output as compared to the

receiver input. Thus the effectiveness of the AGC system is best revealed by a graph showing the IF amplifier output level (in relative dB) plotted vs the receiver input level (in dBm). The input signal should be an unmodulated sinusoid at the frequency of tuning, whose amplitude is varied in steps from receiver threshold (see Sec.2.1) to front-end saturation (Sec. 2.2.3.1).

3.4.2 Measurement of AGC Response Times

Whereas the AGC tracking test displays the static response of the AGC system, the test to be described will investigate the dynamic, closed-loop response of this system.

The test is best carried out by driving the receiver with a carrier at the frequency of tuning which is amplitude-modulated by a low-frequency square wave. The IF amplifier output is observed on an oscilloscope whose vertical amplifier must be capable of handling signals at the intermediate frequency.* The sweep should be triggered from the square wave generator, and the sweep duration should equal the period of the square wave. Thus the response of the AGC-ed receiver to both a sudden rise and drop of the signal will be apparent from the envelope of the displayed signal. Frequently the "attack" (rise) time constant will differ from the "recovery" (fall) time constant, and both should be measured. The dynamic response may also depend upon both of the signal amplitudes which alternately exist at the receiver input, and various combinations of these amplitudes should be tried.

---

* This method is better than one using an AM detector which would introduce an extraneous time constant into the measurement.

4. MEASUREMENT OF INTERMODULATION DISTORTION IN FDM TELEMETRY: NOISE LOADING MEASUREMENTS

4.1 Fundamentals of Noise Loading Measurements

The measurement of overall intermodulation distortion in a telemetry system is best made by connecting the output of the transmitter via an attenuator to the input of the receiver. (This, of course, will not take into account the distortion caused by the antenna feeders and the propagation medium.) Then all but one of the data channels are fed with appropriate signals and the output power of the empty channel is measured. Since the output from the empty channel is only intermodulation distortion (assuming negligible interchannel crosstalk), one can compute an intermodulation noise-to-signal power ratio (I/S ratio) for the particular data channel by dividing the measurement obtained in the unloaded channel by the signal power measured when the particular data channel is fully loaded. From the measurements of the I/S ratio for each channel a bar graph can be plotted showing the I/S ratio versus the frequency location of the channel in the video spectrum.

In order to simplify and standardize the measurement of intermodulation noise, the video signal at the input to the FM modulator is conveniently simulated by a gaussian noise process covering the bandwidth of the video signal. It can be shown that the statistical properties of gaussian noise are very similar to a complex multichannel (FDM) video signal. Thus it is meaningful to simulate the video signal in a telemetry system by a gaussian process. When this noise-loading technique is used, it is necessary to shape the power-density spectrum of the applied noise signal with a filter so that the resulting signal has approximately the same power-density spectrum as the actual video signal.

Figure 6 shows a block diagram of the noise-loading technique. In order that the intermodulation distortion noise at the demodulator output be measured, an "empty channel" has to be simulated in the input spectrum by a narrowband reject filter (see Fig. 7). The power measured in a corresponding narrow bandpass filter at the output constitutes the intermodulation distortion noise power. By switching out the reject filter it is possible to measure the signal power in the bandpass filter and compute the I/S ratio. If this measurement is performed for different video frequencies a curve of I/S density ratio vs video frequency can be constructed as shown in Fig. 8. This curve exhibits the increased intermodulation noise with video frequency commonly encountered in FM systems.

In addition to being analytically convenient, the noise-loading approach greatly simplifies experimental verification. Intermodulation distortion tests can be standardized and the measurements easily reproduced. In contrast,

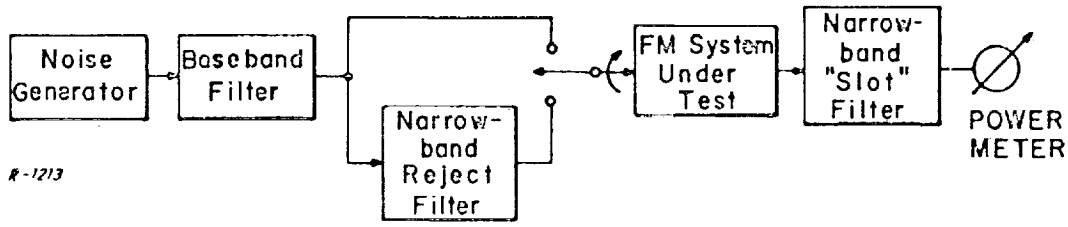

Fig. 6 Noise-Loading Technique for Measurement of Intermodulation Distortion

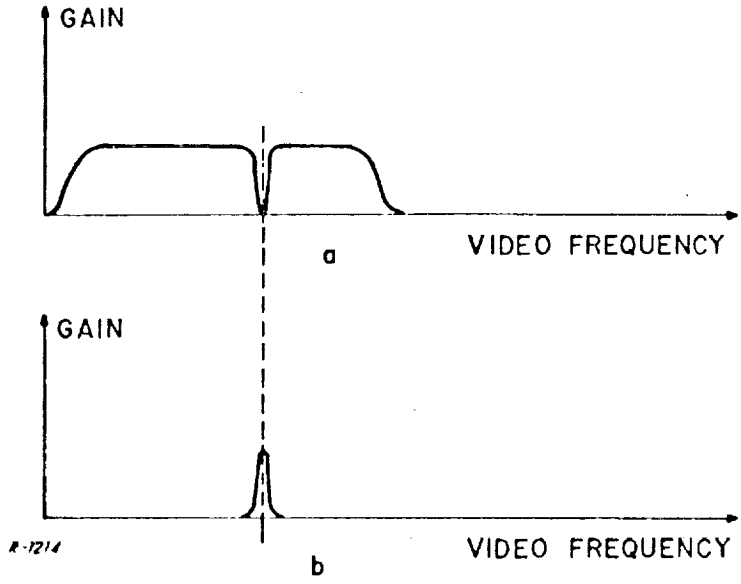

Fig. 7 a) Amplitude Characteristic of Spectral-Shaping Filter for the Noise-Loading Technique

b) Amplitude Characteristic of Narrowband "Slot" Filter

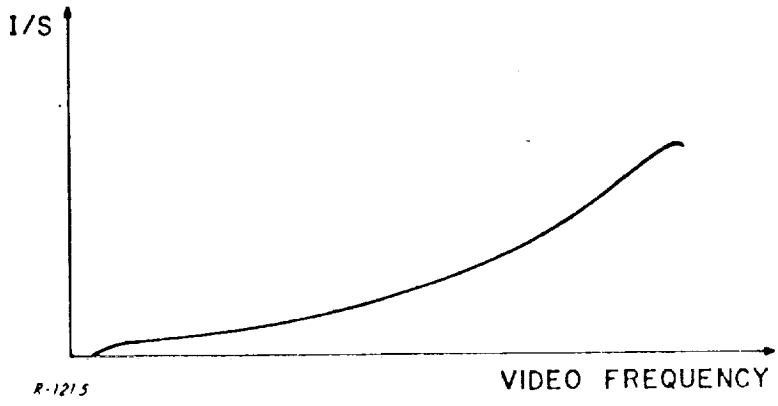

Fig. 8 Typical Curve of Intermodulation Noise-to-Signal Ratio vs Video Frequency

the customary method of simulating the video signal by two or more unmodulated subcarriers is inadequate since it does not reveal higher order intermodulation effects. Moreover, the tone tests are mathematically intractable (except in the trivial case of one or two subcarriers) as well as experimentally cumbersome when more than two tones are used.

4.2 Description of Measurement Configuration

The technique recommended for measuring intermodulation distortion in telemetry receivers is the noise-loading technique shown in Fig. 9. Distortion is measured by simulating a fully loaded telemetry video signal by a noise spectrum having a rectangular shape. This video spectrum contains a notch simulating an empty channel in which the intermodulation distortion is measured after processing through the telemetry system under test.

The block diagram of the intermodulation distortion measurement configuration shown in Fig. 9 uses a white noise generator output passed through a lowpass filter to shape the noise and simulate the video spectrum used with telemetry systems. The video spectrum is passed through an amplifier for gain and isolation, then through a notch filter which places a narrow, deep notch in the video spectrum. Figure 10 illustrates the shape of the resultant video spectrum using various notches. The video filter has a flat response with a 3 dB bandwidth at 85 kHz and an 18 dB per octave roll-off as specified in the IRIG Telemetry Standards[5]. Four different notch filters are used, centered at 10 kHz, 30 kHz, 50 kHz, and 80 kHz which permit measurement of the distortion at four points in the video band.

The shaped video signal is then applied as the modulation signal to the FM modulator and the resulting FM signal processed through the

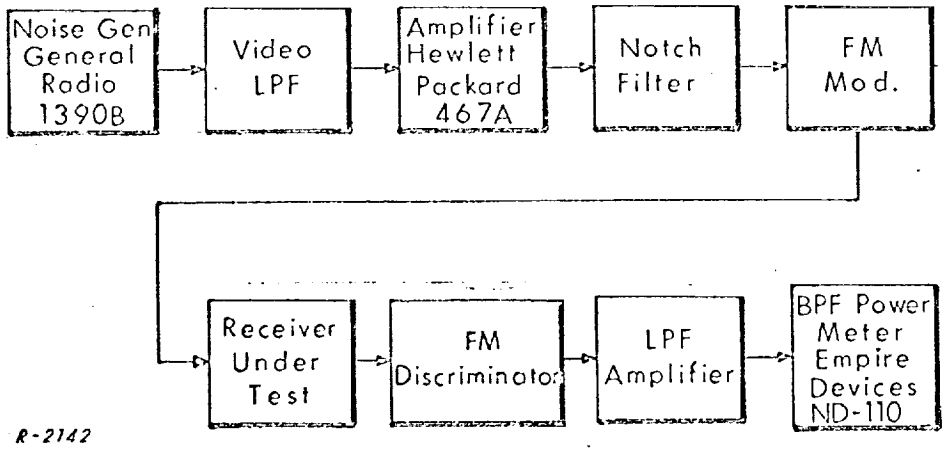

Fig. 9 Block Diagram of Intermodulation Measurement Configuration

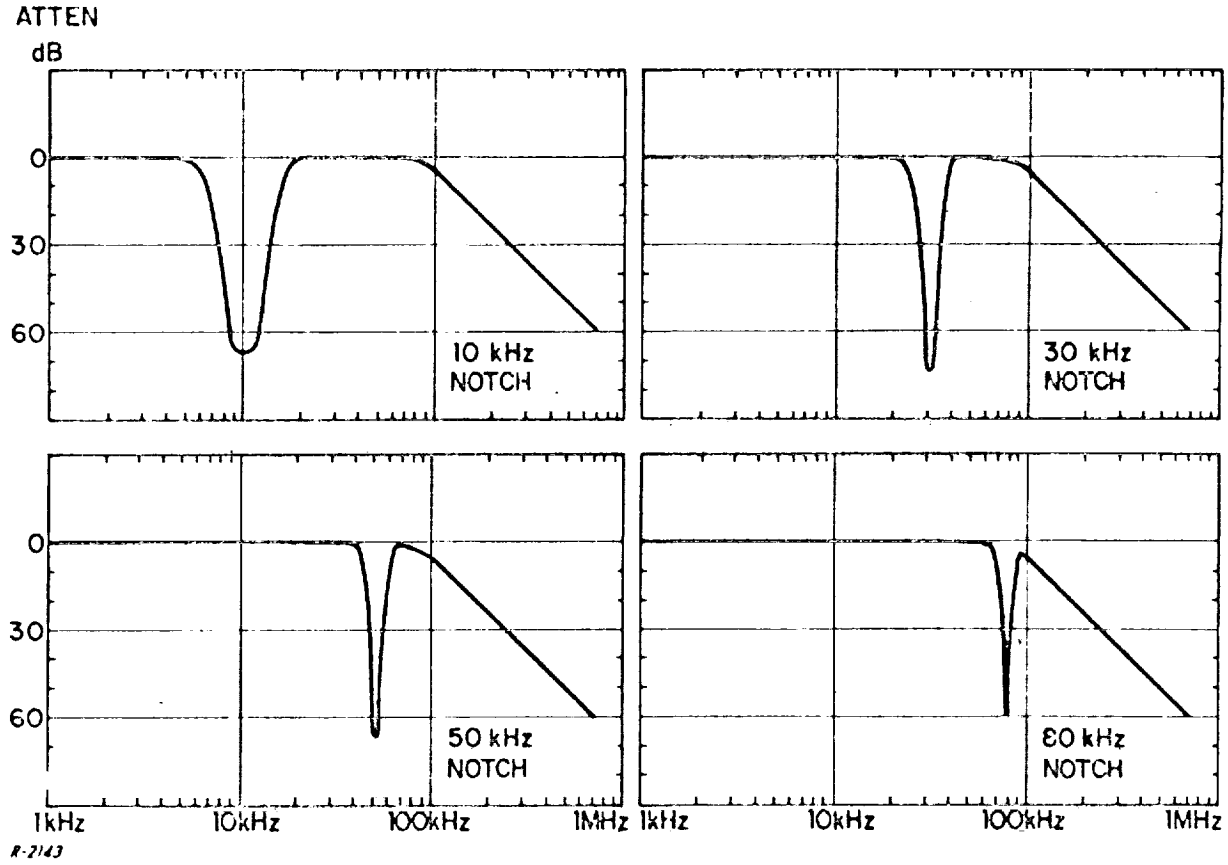

Fig. 10 Simulated Video Spectrum with Empty Channel

predetection filter of the receiver under test. Intermodulation distortion results from the nonlinear signal processing of the video signal. The FM signal at the receiver is then demodulated by the discriminator whose output contains the baseband signal with the distortion introduced in the receiver. The detected signal is passed through a lowpass filter-amplifier to attenuate any RF signals at the discriminator output, and then applied to a tunable bandpass filter, tuned to the notch-filter center frequency and having a somewhat narrower bandwidth than the notch. The output of the bandpass filter is applied to a power meter which then measures the amount of distortion power in the notch.

If the noise notch filter at the input is bypassed then a measurement of signal power at the location of the notch can be taken and a ratio of intermodulation distortion power to signal power (I/S) can be formed.

4.3 Description of Special Test Equipment

Much of the equipment needed for distortion measurements is standard laboratory equipment. These are indicated in Fig. 9 by manufacturer and model number. The lowpass filter used to shape the baseband spectrum is a simple 3-pole Butterworth filter.

Notch filters with the necessary specifications are not readily available and a suitable filter may have to be designed and built. Since it is necessary to measure the I/S as a function of the position of the notch, the filters should be tunable. The depth of the notch filter sets the lower limit to the measurement of distortion since distortion products less than the notch attenuation would be indistinguishable from noise passed by the notch filter. For most measurements attenuations of 70 dB are achievable and adequate since the distortion of interest usually exceeds the -70 dB level.

The lowpass filter-amplifier which follows the discriminator is used only to eliminate the carrier component which is present at the output of the discriminator. The filter therefore should have a 3 dB cutoff frequency above the highest baseband frequency. This filter will not contribute non-linear distortion products, but will introduce some phase distortion across the entire baseband spectrum.

The tunable-bandpass noise meter is a test unit containing a crystal filter and a true-power meter shown in Fig. 11. The filter bandwidth should be slightly narrower than the notch filter so that only distortion and no signal is measured when tuned to the notch frequency. This bandpass filter should be tunable over the noise baseband range.

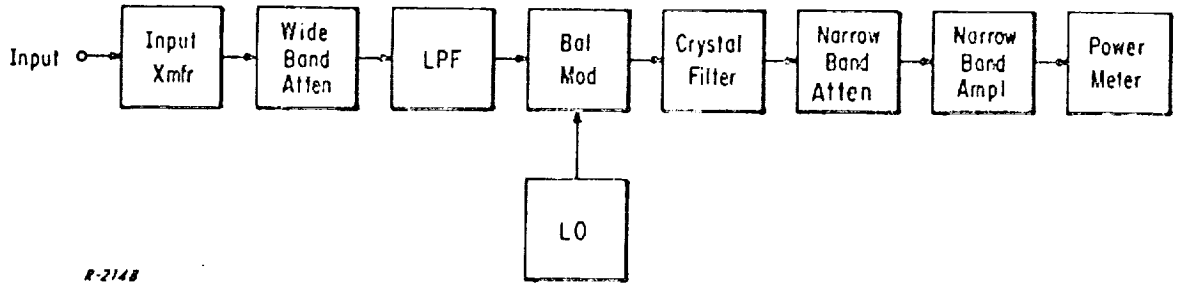

Fig. 11 Block Diagram of Empire Devices Bandpass Noise Meter

4.4 Accumulation of Distortion in the Measurement Configuration

The mechanism for the accumulation of distortion in various parts of the receiver and measurement configuration is of central interest. When an FM modulated signal passes through identical cascaded IF filters, the distortions are highly correlated and add as voltages. In the case where the distortions are not introduced by identical operations, such as with a cascade of a modem and a filter, the individual distortions are uncorrelated and add as powers.

A nomograph which facilitates the computation of distortion accumulation is shown in Fig. 12 for both voltage and power addition. This curve relates the distortion power, in dB, from each of two sources to the total distortion from both sources combined. It permits computation of one of the three distortions involved; i. e., either of the two individual, or the total distortion.

For example, consider the case of the cascade of a predetection IF filter and modem. The distortion in dB from the modem alone can be measured by removing the filter from the measurement configuration, but the filter distortion can only be measured in combination with the modem. Thus, two measurements are necessary in order to isolate the individual contributions. First, the distortion in dB using only the modem is measured and then the distortion in dB using both the modem and filter. The distortion introduced by the filter can then be found by using Fig. 12. Since the distortions are uncorrelated, curve a is applicable. The distortion in dB with the modem (P_1) is subtracted from the total distortion (P_T) and this difference ($P_T - P_1$) is used to enter the ordinate of Fig. 12. The intercept of this difference with curve a gives a point on the abscissa which corresponds to the difference in dB between the individual distortions of the modem and filter ($P_2 - P_1$). If now the distortion with the modem (P_1) is added to this difference, the distortion in dB of the filter alone (P_2) is obtained. The difference ($P_2 - P_1$) can be either positive or negative decibels depending upon whether the difference between the measurements ($P_T - P_1$) is greater than or less than 3 dB. This causes no difficulties. Similar computations can be made for a cascade of identical filters using curve b.

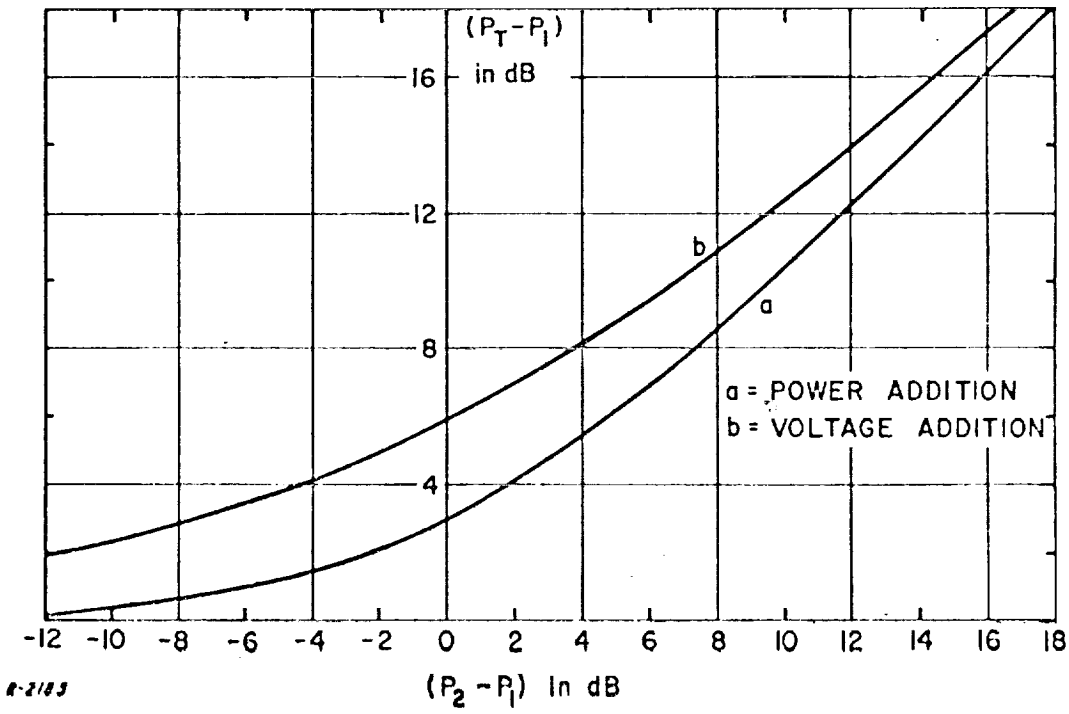

Fig. 12 Nomograph for Accumulation of Distortion

4.5 Measurement Limitations

Limitations to the measurement of distortion in predetection IF filters arise from the masking of this distortion by other disturbances in the measurement configuration. Masking can occur in two ways. The first occurs when the notch filter is too shallow so that noise passing through the notch adds to the distortion generated in the predetection filter. This limitation may be negligible if the notch depth is well below the anticipated predetection IF filter distortions. The second occurs because the FM modulator and discriminator are not perfectly linear and as a result introduce intermodulation distortion of their own. As long as this distortion does not overwhelm the distortion from the predetection filters no significant problem exists, because we can use the nomograph of Fig. 12 to isolate filter distortion from the overall distortion measurement.

Before proceeding with the measurement of distortion in predetection IF filters, it is first necessary to measure the residual distortion introduced in the measurement configuration in order to establish its noise floor, i.e., the lower limit to I/S distortion. Figure 13 shows the test setup for each of four noise-floor measurements. Part A of Fig. 13 shows the equipment arrangement for measuring the residual distortion caused by the notch filter and baseband shaping circuits.

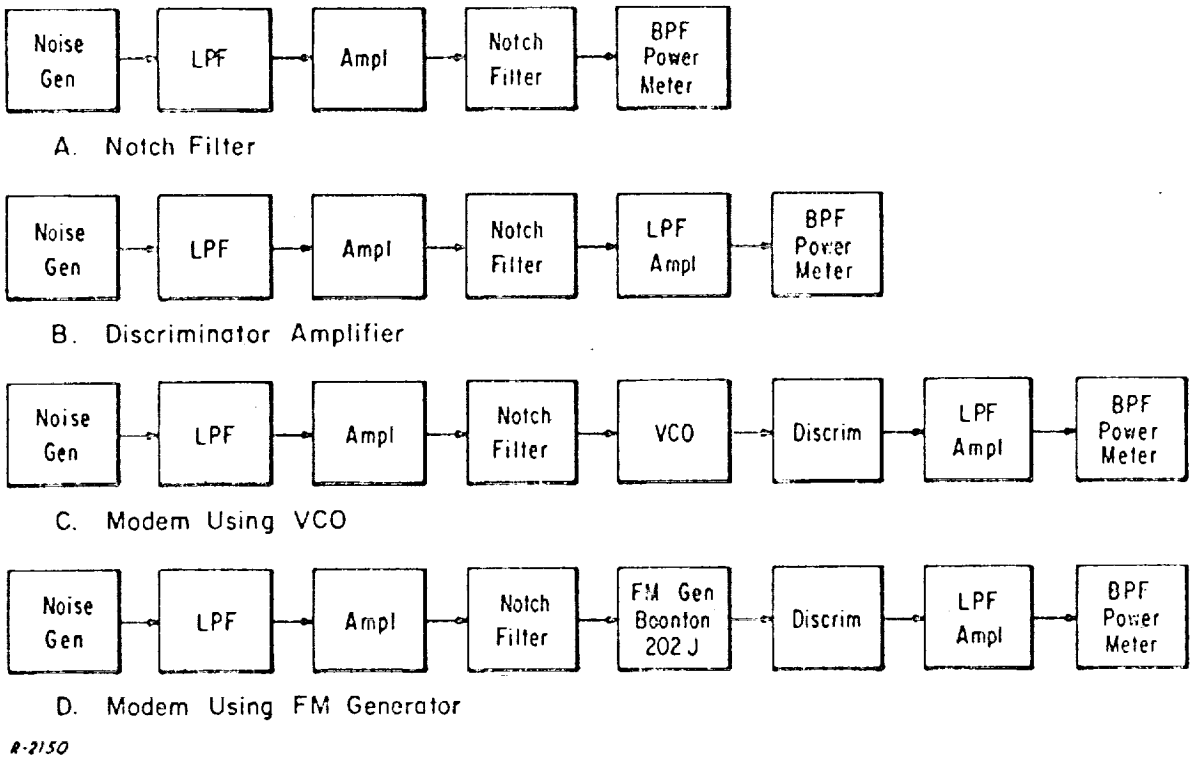

Fig. 13 Test for Identifying Contributions to the Residual Distortion

In Part B, the spectrum-shaping circuits plus the amplifier-filter following the discriminator are evaluated. A small increase in distortion usually is experienced due to unavoidable noise generated in the amplifier. Both of these noise floors should be quite low relative to the greater distortions usually encountered in most telemetry receivers.

Part C of Fig. 13 shows the measurement of the noise floor for the entire test system using a notch filter tuned to the high end of the baseband range. Positioning the filter there will yield the highest distortion readings since it is at the high end of the video spectrum.

In order to maintain a constant level into the power meter an attenuator should be inserted between the amplifier-filter and the bandpass filter-power meter. As the FM deviation is changed, this attenuator should be changed keeping the level at the power meter constant.

An example of a typical noise-loading distortion curve is shown in Fig. 14. The lower curve in Fig. 14 shows the effect of the attenuator setting on the noise floor with no baseband modulation on the VCO. In effect this curve plots the noise level measured at the power meter resulting from

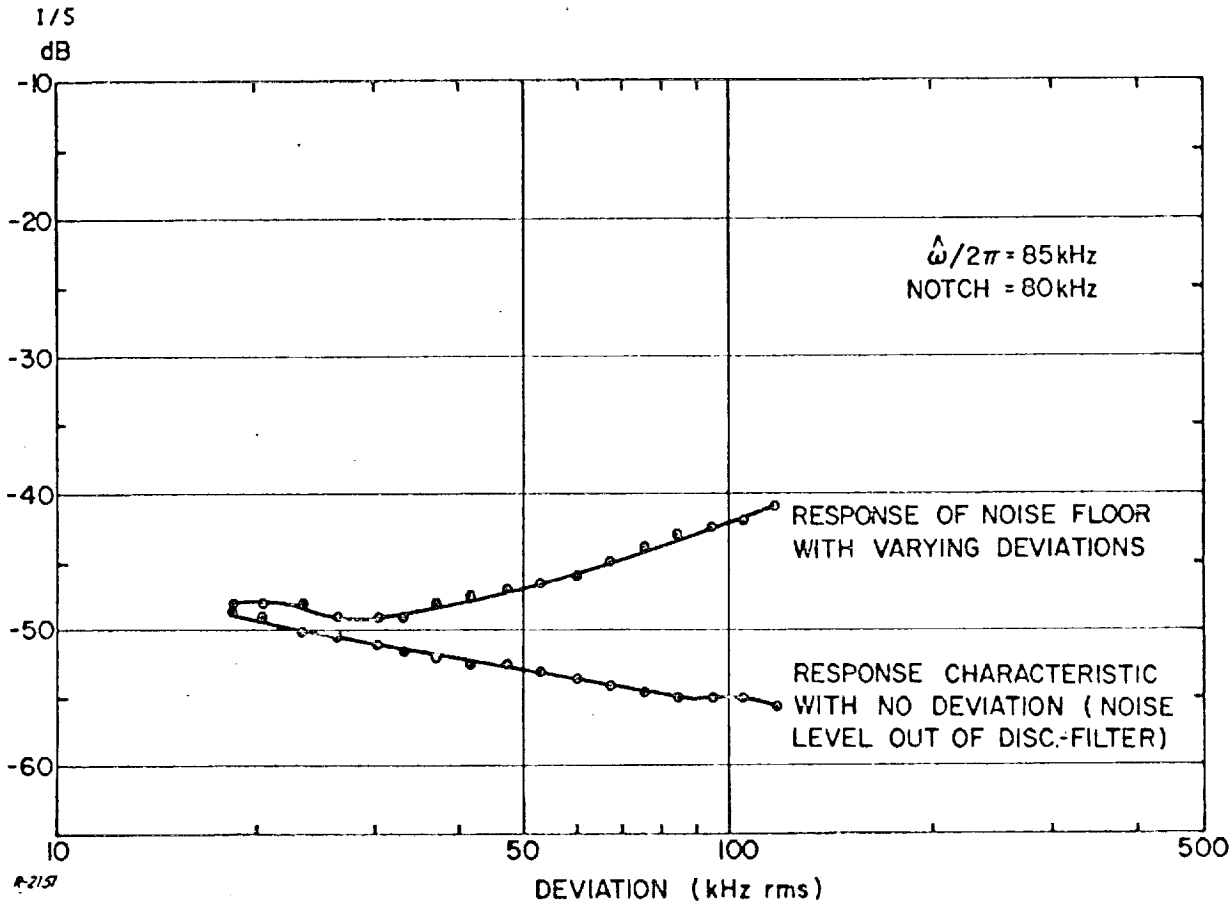

Fig. 14 Noise Floor vs Deviation

decreasing the attenuation of this noise. The noise measured here is generated in the discriminator and amplifier-filter. As is to be expected, it is highest at the low attenuator settings, corresponding to the low deviations and may place some limitations in measuring the distortion effects of wideband predetection filters in the case of low deviations since the distortion from the filter would be low.

The upper curve in Fig. 14 is a plot of actual noise floor of a telemetry system as a function of deviation. Here the noise floor decreases as the deviation decreases. This kind of performance is to be expected since the distortion which is principally caused by the VCO-discriminator combination is directly related to modulator characteristic nonlinearities which are necessarily worse at large deviations.

It should be observed that an rms deviation of 53.3 kHz corresponds to a reading of 125 kHz peak deviation on the telemetry receiver deviation meter which is the recommended peak deviation for telemetry operation in the IRIG telemetry standards. At 53.3 kHz deviation the system noise floor was -47 dB. This means distortions much less than -47 dB cannot be measured. However, this floor happened to be low enough to permit measurement of the I/S in predetection IF filters. This noise floor can be reduced even further by utilizing a more linear VCO or discriminator characteristic.

Part D of Fig. 13 is a setup using a standard FM generator rather than the linear VCO modulator. This generator has a nonlinearity specification of less than 1.5% deviation from a straight line. With this generator the noise floor is increased to -39 dB, which demonstrates the need for good linearity in the FM modulator as compared to the more linear VCO. The superior linearity of the VCO is obvious and is reflected in lower distortion measurements.

5. MEASUREMENT OF CAPTURE PERFORMANCE IN FM RECEIVERS

In general, measurement of capture performance directly in terms of a signal quality performance index (e.g., the probability of error) most suited to the desired application is an unwieldy and often unfeasible operation. It is therefore desirable to perform the measurements in terms of some standard and easily identifiable, separable and measurable modulation waveforms (such as single tones). The measured characteristic of the desired modulation should then be portrayed along with a corresponding measure of the attendant distortion, both as functions of the signal amplitude ratio. The resulting quantities could then be related, by means of a separate and independent computation or measurement, to error probability or some other performance index that is appropriate to a specific application. In this way, the receiver capture performance measurements can be standardized for all possible applications. Only the interpretation of the results in specific circumstances remains, and this is legitimately left to the discretion of the user, not the salesman or the manufacturer. The user may then abstract the capture performance of the receiver by a single number -- the capture ratio -- which he determines from the standard capture performance curves on the basis of a criterion of capture threshold that is most suitable to the specific intended application.

5.1 Procedure for Measuring General Capture Characteristics

A complete description of the capture performance of an FM receiver from the viewpoint of a specified application requires the presentation of either

a) a plot of the variation of a suitable measure of the desired baseband signal component plus a plot of a correspondingly appropriate measure of the disturbance introduced in the desired baseband by the interference, both as functions of the interference ratio, or

b) a plot of the ratio of the proper measures of baseband signal and disturbance as a function of the input interference ratio.

The interference used in the test could be derived from an independent source or it could represent a simulated secondary-path replica of the desired signal. We consider first capture performance measurements with two independent FM signal generators, each sinusoidally modulated with distinct tone frequencies as shown in Fig. 15. The frequency deviation of

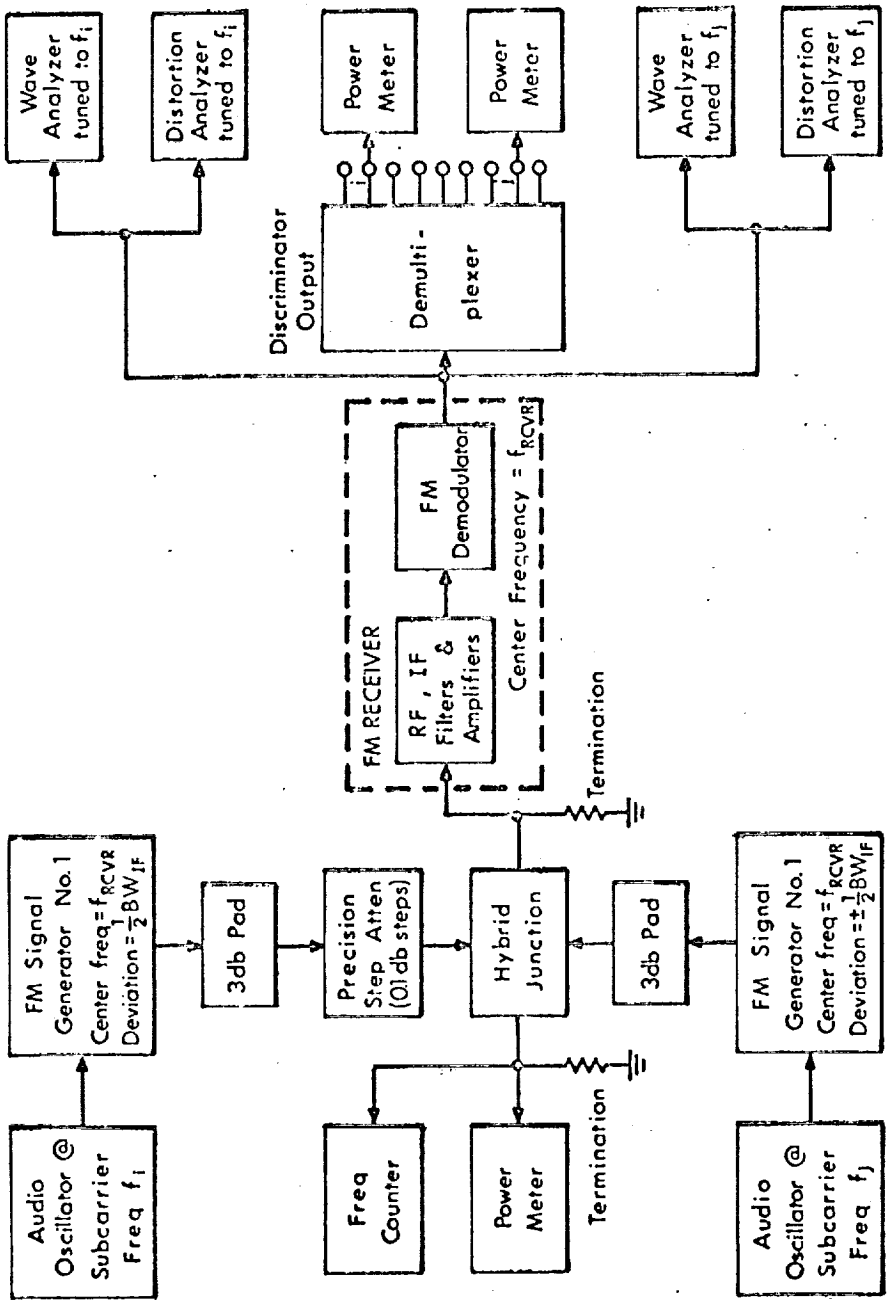

Fig. 15 Equipment Setup for Standardized Measurement of Capture Performance

the desired signal, presumably the stronger, as well as the (weaker) interfering signal, are adjusted to correspond to 100% modulation of the RF carrier. The carriers of the two signals are adjusted to be identical with both tuned to the precise center frequency of the receiver (in particular, the discriminator). The requirements on the carrier frequency adjustment of the two signals are dictated by the dependence of capture performance measurements upon the average difference between the instantaneous frequencies of the two input FM signals and upon the percent-of-time distribution of the instantaneous frequency difference. These characteristics of the instantaneous frequency depend upon the difference between the nominal carriers of the FM signals as well as the individual modulations of the input signals.

An important initial step in the capture performance test procedure is to decide on a convenient input signal level. Two considerations enter into a choice of a signal level. It should be recalled that the instantaneous amplitude of the resultant of two CW signals varies from a minimum of $E_S(1-a)$ to a maximum of $E_S(1+a)$, where E_S is the amplitude of the stronger signal and a is the interference ratio (or ratio of weaker-to-stronger signal amplitude). The maximum permissible value of E_S is determined by the requirement that a signal amplitude of $2E_S$ (which will be encountered when $\underline{a} = 1$) not drive the linear receiver stages into saturation.

The second preliminary step is to equalize the carrier frequencies of the two input FM signals and to center them in the receiver passband. This may be achieved with a frequency counter or by centering one unmodulated signal generator carrier at the center frequency of the discriminator and adjusting the frequency of the other unmodulated signal generator for a zero beat as observed by the detected spike pattern in the output of the discriminator. A sketch of a typical spike pattern is illustrated in Fig. 16. It is important during the capture performance tests that the relative carrier frequency drift be held to a small fraction of the lowpass bandwidth in the output of the discriminator. This usually forces a requirement of no more than 1 kc relative drift between the FM signals during the test.

In performing the capture tests, it is necessary to monitor accurately the level of both signals at the receiver front end. The amplitude of one signal will be varied relative to the other in incremental steps of 0.1 db in order to provide a detailed investigation of the capture transition region. This region typically covers a range of relative signal levels of 3-10 db depending upon the particular receiver design. An initial equalization of amplitude is therefore required with an accurately calibrated power meter or, more precisely, by observing the spike pattern in the output of the discriminator during the "zero beat" frequency equalization operation. The amplitude of one

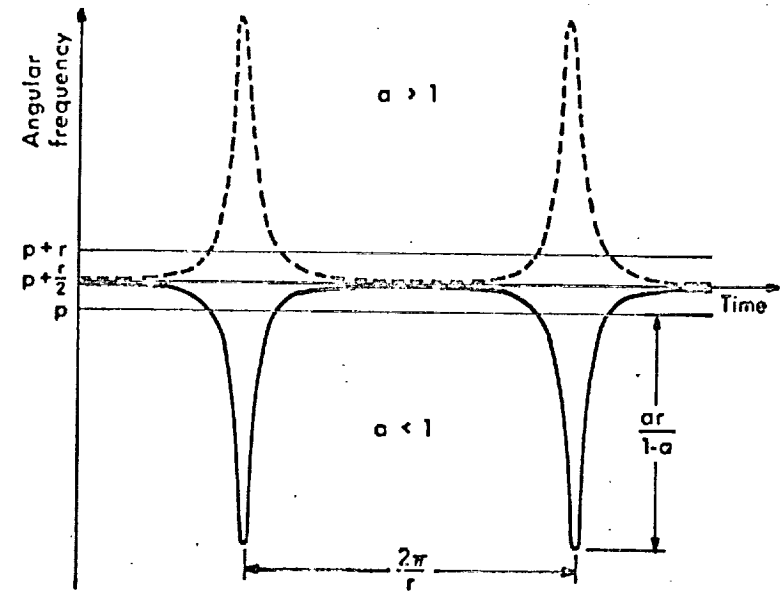

Fig. 16 FM Disturbance Pattern Caused by Two-Carrier Interference, Plotted for a = 0.8 and a = 1/0.8.
p = frequency of stronger signal
p + r = frequency of weaker signal

unmodulated carrier input is adjusted so that the observed discriminator spike pattern reverses polarity. At the setting of the relative amplitude for which this polarity reversal occurs the two generators are equalized in amplitude. The frequency of the interfering generator is then adjusted by "zero beating" the observed frequency spike pattern since it usually is necessary to offset carrier frequencies slightly to facilitate detection of an abrupt polarity reversal. After the amplitudes have been equalized, a step attenuator can be varied to adjust the amplitudes of the FM signals to the desired interference ratio.

The capture performance measurements proceed after the two signal generators have been calibrated in amplitude and frequency. Each generator is sinusoidally modulated by a different audio frequency with equal frequency deviations corresponding to the maximum deviation of the desired signal modulation. The output of the discriminator is applied to two wave analyzers and two distortion analyzers. The observed strength of each output tone corresponding to the sinusoidal stronger and weaker signal modulated is plotted in per cent of its undisturbed would-be value in the absence of the signal carrying the other tone. The total attendant distortion accompanying each tone

is also plotted against the corresponding values of the input signal amplitude ratio, a (marked on a logarithmic horizontal scale). The so-called "total attendant distortion" includes the tone of the other signal.

The capture curves obtained by this procedure should portray symmetry about the line a = 1. Furthermore, the crossover point in the capture transition region should occur at a = 1. Crossovers occurring for a different value of a indicate an error in equalizing the signal generator levels in the preliminary calibration test. A misalignment in signal generator frequency, however, will affect the width of the capture transition region and the output distortion level.

Typical stronger-signal and weaker-signal capture characteristics (excluding the "total attendant distortion" curves to avoid crowding) are shown in Fig. 17. A medium-quality FM receiver, operating in the presence of co-channel interference, is likely to have the capture characteristics marked A and A'. The plot of "total attendant distortion" associated with A would rise to noticeable values as A begins to show a drop and would continue to rise toward a saturation value given by the level of the pure tone of the interfering signal as a is made considerably greater than unity. The amplitude ratio a_{cap} is arbitrarily designated the capture ratio of the receiver and it is

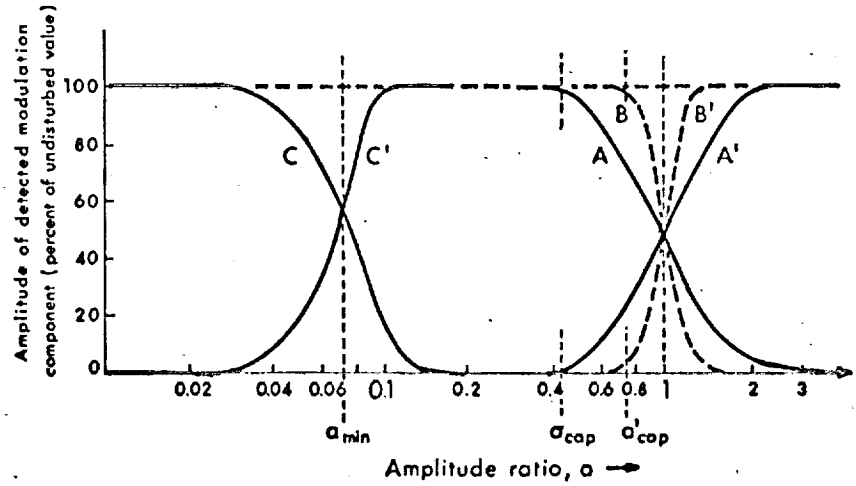

R-5708

Fig. 17 Typical Capture Characteristics for an FM Receiver
A and A' Describe Likely Stronger-Signal Capture Performance
B and B' Describe Performance of Same Receiver with a Stronger-Signal-Capture-Improvement Operation Added to its Circuit
C and C' Result from Addition of a Weaker-Signal Capture Device

a function of the receiver design as well as the type of interference (co-channel or otherwise) for which it is measured, and the maximum tolerable level of disturbance in the intended application. If a stronger-signal enhancement circuit (for example, one or more narrow-band limiters, or a feedforward circuit, etc.) is switched into the signal path in the receiver, the A curves are transformed into curves such as the B curves. The A and B curves, of course, continue at the 100 per cent level outside the region shown, although they are stopped in the figure below $a = a_{cap}$. The introduction of a weaker-signal capture circuit leads to characteristics such as C and C'. The C and C' curves usually merge into curves such as the A or B curves around $\underline{a} = 1$.

It is clear from Fig. 17 that improvements in the stronger-signal capture ability of the receiver result in a narrowing of the capture transition range ($a_{cap} < a < 1/a_{cap}$), or the range of values of the amplitude difference between two competing signals in which the receiver is unable to deliver the message of either signal without harmful disturbance from the other.

5.2 Procedure for Measuring Two-Path Capture Tests in FDM/FM

In FDM/FM telemetry reception, the capture performance against a secondary-path replica of the desired signal is of special interest. Thus, in place of an independent RF interfering signal, the capture test on the FDM/FM receiver is conducted using an interfering signal which is an attenuated and delayed replica of the desired signal. Both the amplitude ratio and delay difference between the two replicas of the desired signal become capture test parameters. The test is simplified by considering only the largest expected delay difference, τ_d, since for values of τ_d up to a few tens of microseconds, the baseband disturbances rise monotonically with τ_d.

In order to characterize capture performance in the manner most immediately applicable to the needs of the telemetry user it is necessary to choose baseband test signals that are representative of telemetry subchannel signals. For slowly varying data channels, unmodulated subcarriers closely approximate the actual modulated subcarriers. For the more rapidly varying data channels, such as vibration data, particularly where SSB is used in the subchannels, bands of noise in the test subchannels may provide a more appropriate model.

The detected baseband signal appearing in the output of the demodulator must also be evaluated in a manner which conclusively demonstrates telemetry system performance. In particular, capture transition distortion accompanying the detected baseband signal must be measured ahd characterized by methods which best demonstrate the overall effect upon baseband

detection of the multichannel telemetry signal. In FDM/FM systems, baseband intermodulation distortion is the principal index of performance.

A typical setup for performing capture tests on an FDM/FM telemetry receiver is illustrated in Fig. 18. The desired FDM/FM telemetry signal is derived from a telemetry transmitter which matches the characteristics of the receiver under test. The choice of a baseband test signal used in the transmitter and the method of evaluation will be discussed in greater detail later on. The output of the transmitter is adjusted for some convenient power level, say one watt. The simulated multipath interference signal is derived by passing the RF signal through two separate channels between the transmitter and the receiver. One channel, identified as the desired signal, is essentially a direct path. The other channel, identified as the secondary-path signal channel, contains both a variable attenuator and a variable delay line. A fixed delay line is also incorporated in the direct channel to facilitate delay control if it is desirable to study the effects of relative delay between the two channels for both small and large values of delay. It is important in all of these connections that cable lengths be short and that properly matched transmission line connections and terminations be provided in order to ensure that reflections are kept to a negligible level. In splitting the signal into two mutually independent channels, hybrid junctions (or hybrid wave-guide rings) are used both to achieve a signal split and to recombine the two signal paths.

The variable phase shifter must have a linear phase shift versus frequency characteristic. Typical of such a device is a calibrated coaxial line stretcher. Used as a delay line in this manner, these transmission line devices cover a wide range of operating frequencies from VHF well into S-band. For precise delay measurements, however, it is necessary to have an accurate indication of line length.

The difference signal is monitored in the output of the hybrid junction. The signal levels are first equalized by adjusting the attenuation in one of the signal paths for a null as indicated by the power meter. The variable attenuator in the "multipath" channel is then adjusted to achieve the desired relative signal amplitude. Because of identical carrier frequencies, it is permissible to adjust the amplitudes at the input to the receiver in this manner without being concerned about ripple in the receiver filters which upsets accurate amplitude calibration between the two signals. It should be recalled that an accurate amplitude balance of the signals prior to demodulation was an essential operation in the previous capture tests on the FM demodulator. Balancing in the output of the hybrid junction is sufficient for the multipath capture tests described here.

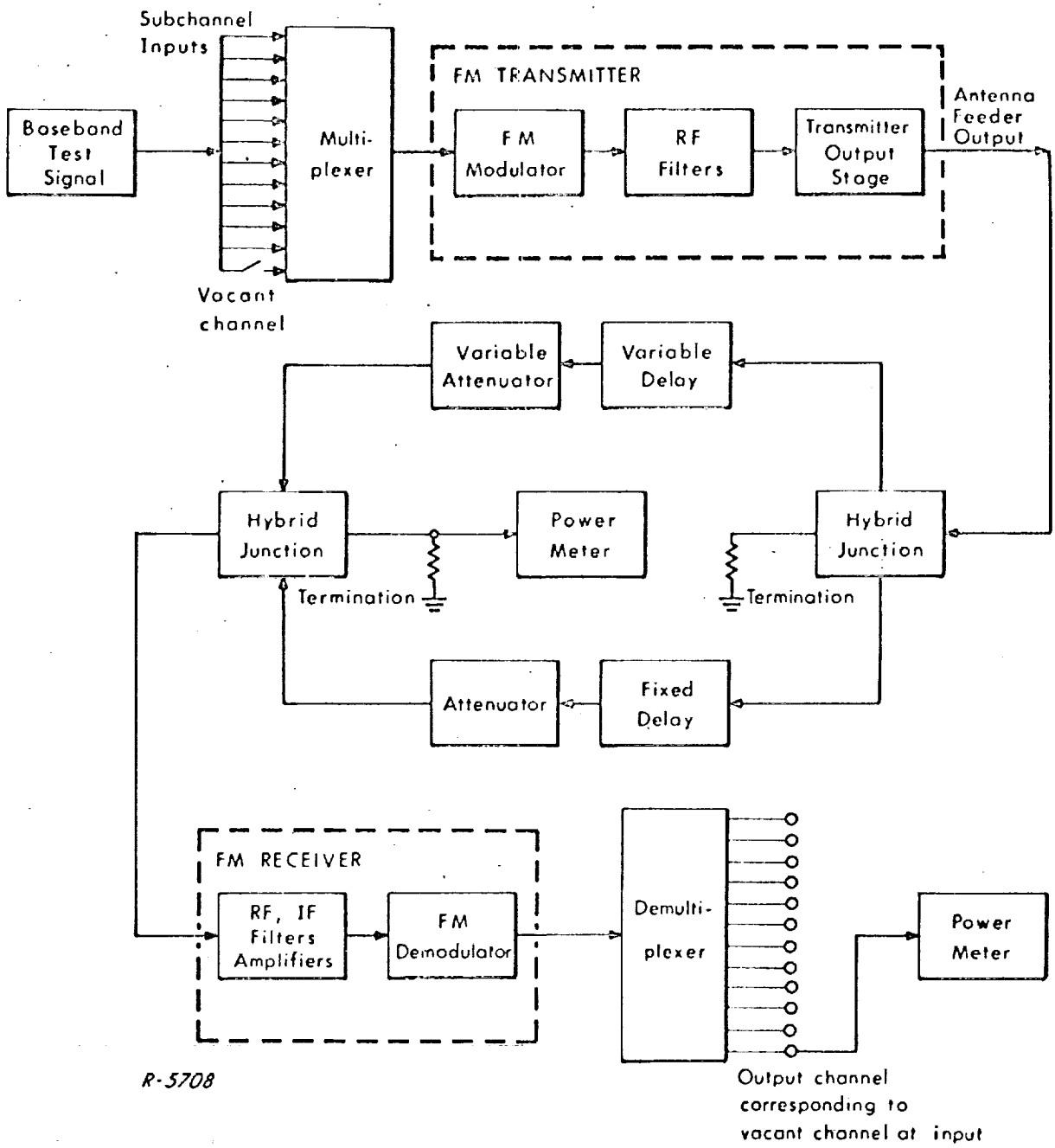

Fig. 18 Block Diagram of Multipath Capture Test on FDM/FM Telemetry Receiver

The important sources of baseband disturbance in FDM/FM telemetry systems can be classified into three groups:

a) additive noise at the receiver input,

b) intermodulation distortion noise, and

c) interchannel crosstalk.

In the capture tests, the signal levels must be adjusted so that the input signal strength is well above the random-noise threshold of the receiver.

Intermodulation distortion noise is caused by nonlinearities in the system. By nonlinearity we mean here any operation which creates spectral components in the output that were absent at the input. The following sources of intermodulation (distortion) noise may occur in an FM system:

a) amplitude nonlinearities in baseband and multiplex circuits,

b) FM modulator nonlinearity,

c) RF and IF filtering at the receiver or transmitter,

d) antenna feeder mismatch at the transmitter or receiver,

e) multipath and scatter effects in the propagation medium (e.g., frequency selective fading),

f) FM demodulator nonlinearity, and

g) FM demodulator operation below its noise threshold.

The intermodulation noise in a subchannel is very much dependent (in a complicated way) on the signals in all the other subchannels and will essentially vanish if all other subchannels are empty.

Interchannel crosstalk is not caused by nonlinear effects, but by insufficient channel filtering in the multiplexer and demultiplexer circuits. It consists mainly of components from the two adjacent subchannels which are not sufficiently attenuated by the filter of the observec subchannel. Thus, as with intermodulation noise, the interchannel crosstalk is absent when all subchannels are empty. The interchannel crosstalk is easily separated from intermodulation noise by placing the multiplexer back to back with the demultiplexer and only loading the two subchannels adjacent to the observed

subchannel. Under that condition the intermodulation noise is negligible. By using sufficiently sharp subchannel filters it is possible to reduce the interchannel crosstalk to a negligible level.

A conclusive measurement of residual intermodulation noise in an FDM/FM system may be made by connecting the output of the transmitter via an attenuator to the input of the receiver. This measurement does not take into account the distortion caused by the antenna feeders or the propagation medium. All but one of the subchannels are then fed with appropriate signals and the output power of the empty channel is measured. Since the output from the empty channel is due only to intermodulation (assuming interchannel crosstalk absent), one can compute an intermodulation noise-to-signal power ratio (I/S ratio) for the particular subchannel by dividing by the signal power which is measured when the particular subchannel is fully loaded. From the measurements of the I/S ratio for each subchannel a curve can be produced showing the I/S ratio versus the baseband frequency of the frequency multiplexed subchannels.

A simple measurement of intermodulation noise can be made with the baseband signal at the input to the FM modulator simulated by a gaussian noise source covering the entire telemetry baseband bandwidth. It can be shown that a complex multichannel (FDM) baseband signal has statistical properties that are nearly gaussian. Thus, it is meaningful to simulate the resultant baseband signal in an FDM/FM system by a gaussian noise signal. However, when this so-called noise loading technique is used, it is necessary to shape the power density spectrum of the applied noise signal with a filter so that the resulting signal has approximately the same power density spectrum as the actual baseband signal. The same is true in the noise loading capture tests.

In measuring the intermodulation noise at the demodulator, an "empty channel" is simulated in the input spectrum by disconnecting the particular channel under test from the noise source. The power measured in the corresponding subchannel in the output of the demodulator constitutes the intermodulation noise power. The signal power in the test subchannel output filter can be measured by connecting only that subchannel to the noise source. If this measurement is performed for different baseband frequencies, a curve of I/S ratio versus baseband frequency can be constructed.

After the residual baseband distortion products have been measured, the capture test may proceed. The test baseband signal may be chosen to be a number of tones corresponding to slowly modulated subcarriers at various

frequency positions within assigned channel frequency spaces. If one such tone is used, then the level of one of its harmonics in the output may be taken as a measure of the capture transition distortion as the amplitude ratio of the simulated paths assumes values near unity. More than two tones would allow intermodulation products to be used as measures of capture transition distortion.

For some applications, noise loading of a number of assigned channels is a more appropriate test signal. By properly shaping the noise spectral density, the baseband test signal would approximate very closely a typical wideband-data telemetry multiplex input signal. The level of this baseband test signal may be adjusted to produce the same rms deviation of the FM carrier as produced by the telemetry signal. This baseband noise signal is applied to all but one of the multiplexer input circuits and intermodulation noise power is measured in the output of the vacant channel in the demultiplexer following the FM demodulator. Measurements of output intermodulation distortion are plotted as a function of the multipath interference ratio $\underline{a}$, the differential delay, τ_d, and the baseband center frequency of the test subchannel. Since the main interest is in characterization of capture performance, it is sufficient to measure intermodulation distortion in only one telemetry channel as a function of the amplitude interference ratio $\underline{a}$ and the simulated multipath differential delay, τ_d. It is usually sufficient to characterize the capture performance for only one setting of the multipath delay factor, choosing a delay which represents a worst case condition with regard to the level of intermodulation distortion.

In another form of the test, a noise signal is applied to one particular test subchannel. The frequency deviation of the RF carrier would be adjusted to the deviation normally allowed for the particular subcarrier signal. Noise power in the output of the subchannel filters at the demultiplexer would be measured as a function of the interference ratio $\underline{a}$. Power in the frequency range from zero to twice the test subchannel bandwidth could also be used as a measure of capture intermodulation distortion. This follows from the fact that the spectral effects of nonlinear processing of the test subchannel can be accounted for by convolutions of the assumed test channel spectral density with itself, which produces low frequency components that can be used as a measure of capture performance.

The "capture ratio" of the telemetry receiver may be determined from the curves once a tolerable level of distortion has been established from system user requirements or, equivalently, when the amplitude of the desired signal dips to some critical lower level. The value of $\underline{a}$ for which this occurs

can then be identified as the capture ratio. However, it should be emphasized that such a performance index is subject to several qualifications:

a) specification must be made for a given delay differential;

b) specification must be made with regard to a particular performance criterion such as tolerable level of distortion as determined by user requirements; and

c) specification must be made in terms of standard tests with reference to the same multiplex subchannel.

6. MEASUREMENT OF BIT ERROR RATE AND CLOCK PHASE ERROR IN PCM TELEMETRY

6.1 Introduction

In PCM systems the receiving end of the data modem, sometimes called a Bit Synchronizer, provides the transformation between an analog carrier demodulator and the data and clock outputs. The latter two are binary digital signals (1, 0) which are generally DC logic levels. The input to the bit synchronizer is the appropriate modulated waveform such as PSK, NRZ or split-phase plus the noise output associated with the preceding demodulation and conversion stages. The bit synchronizer generally contains a phase-locked loop for bit sync tracking and a data filter and decision circuit. The performance as observed at the data and clock terminals can best be characterized by binary error rate and clock phase error.

Although the noise at the bit synchronizer input in actual operation will in general not be gaussian, it is customary to evaluate its performance as a subsystem with white gaussian noise. This permits a direct comparison with theoretical performance calculations which are generally available only for gaussian noise conditions. The PLL performance will, of course, depend on both noise and signal dynamics. While white noise is easy to specify through a single parameter -- the noise power density, signal dynamics, on the other hand, as produced, for example, by tape recorder wow and flutter do not lend themselves to easy description and/or simulation. Another factor which often influences the behavior of bit synchronizers is the specific sequence of data bits. For example, long runs of 1's or 0's may cause loss of bit sync with NRZ data due to the absence of bit transitions which provide the input to the PLL.

6.2 Principles of Tester

The test configuration shown in Fig. 19 is designed to evaluate the performance of bit synchronizers for each of the above factors. The system under test, indicated within the dotted lines could be the bit synchronizer itself with an appropriate waveform generator and additive noise source or it could be any combination of complementary receiver and transmitter subsystems terminating in the bit synchronizer. Note that in the configuration shown, test system inputs and outputs are simultaneously accessible at the same place. A later section will be concerned with the situation where a tape recorder or transmission link intervenes between transmitter and receiver.

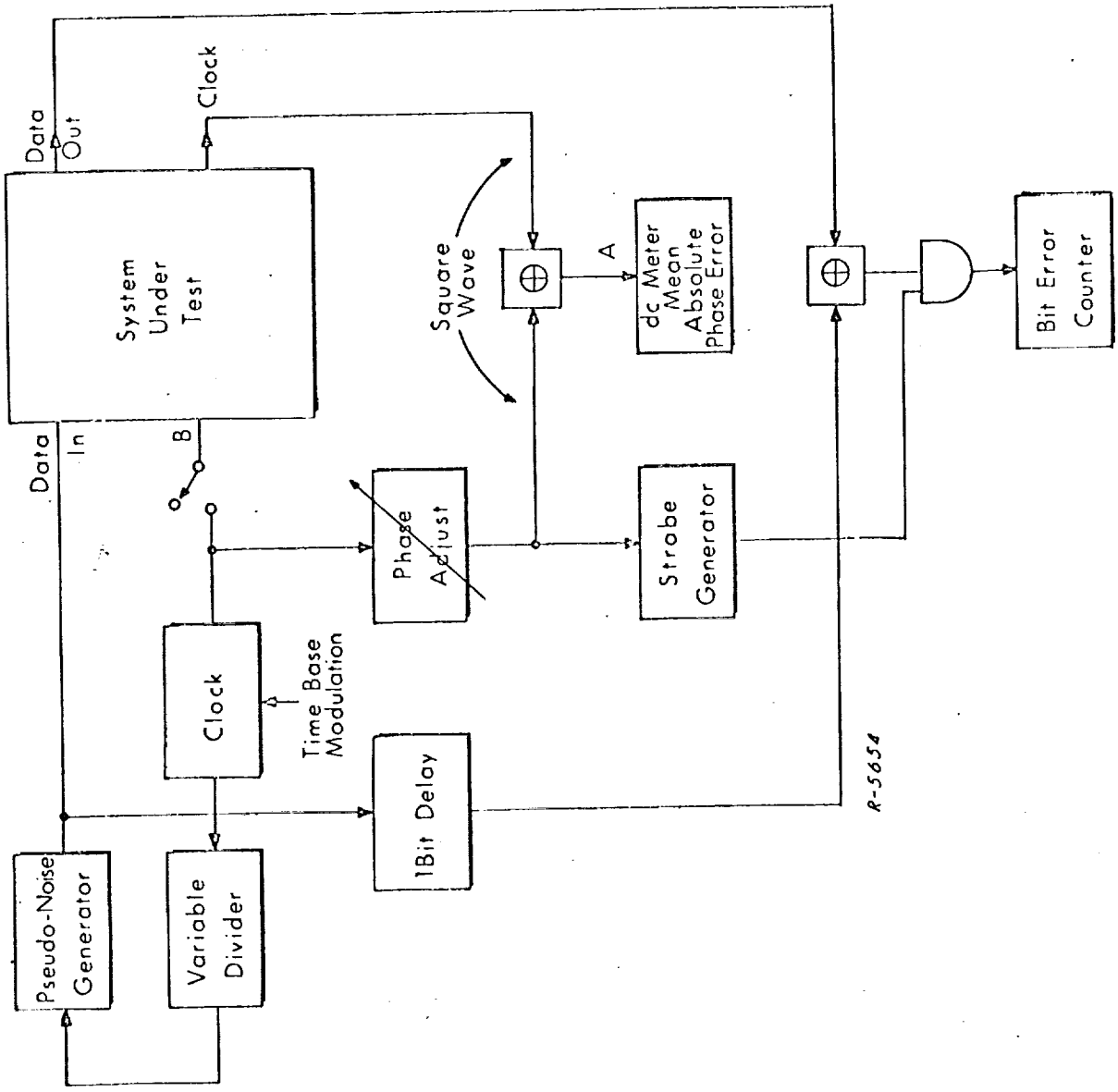

Fig. 19 Bit Error Rate and Clock Phase Error Measurement with Accessible Transmitter

The pseudo noise generator (PNG) is of a conventional type consisting of a feedback shift register connected to produce a maximal length sequence. The data rate for the test is established by the clock frequency and the data transitions are provided by the PNG. The presence of the variable divider between the clock and PNG makes it possible to produce arbitrarily long sequences of 0's and 1's at the PNG output. When the clock is applied to the PNG directly we have the usual PN sequences consisting of all possible occurrences of m bits in succession (except all 0's) where m is the length of the shift register. This imples a maximum run of m 1's. When the variable divider is set for one stage of division, each run of a binary symbol in the original sequence is doubled since the clock is still running at the same rate but the PNG output transitions occur half as often. When the divider is set to divide by four, each run is quadrupled, and so forth.

Time-Base Modulation is shown applied to the clock to simulate instabilities caused by tape recorders or other sources. A simple sinusoidal modulation can be applied and the corresponding phase error amplitude can be observed. This provides a means for testing the closed loop response of the bit-sync PLL.

The clock phase error or, more precisely the mean absolute phase error, whether due to signal dynamics or noise is measured as shown in Fig.19. Two square waves are applied to a mod-2 adder -- one from the transmitter clock and one from the bit synchronizer output. The two square waves are of the form shown in Fig.20 and are phased so that small phase errors yield narrow positive-going pulses at the output of the mod-2 adder. It can be seen that the pulses have the same sign for both positive and negative phase error and their width is proportional to the phase error. Therefore, since the pulses have standard amplitude, their DC level is a measure of the mean absolute phase error. This measure is similar to the mean square phase error in providing an indication of the spread of phase errors, but is considerably simpler to instrument.

In order to offset delays through the system under test a phase adjustment is provided to bring the two square waves into alignment at the start of the experiment. A similar purpose is served by the one bit delay in the data path to the bit error comparator*. Since the decisions are made at the end of a data interval, at least a one bit delay is incurred through the

---

*In the absence of the Variable Divider, the one-bit delay could be derived from the PNG. However, since the PNG may be cycling at a lower rate than the clock, one stage of the shift register does not correspond to one-bit delay.

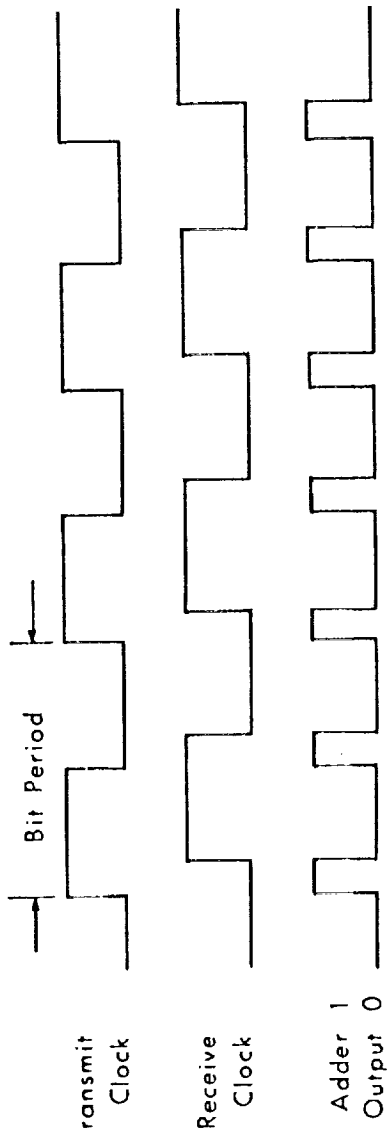

Fig. 20 Phase Meter Waveforms

system under test. Further fractional bit delays can be tolerated as long as the strobe which gates the mod-2 adder output into the Bit Error Counter occurs at an instant where both inputs to the adder pertain to the same data bit. This condition is almost certainly assured since the strobe is derived from the phase shifted clock square-wave.

6.3 Procedure for Measuring Clock Phase Error and Bit Error Rate

1. Assemble test configuration shown in Fig. 19 and connect Data and Clock inputs and outputs to the system under test.

2. Set clock at data rate to be tested. Set signal level at a nominal value, and remove all external additive noise and time base modulation. Set Variable Divider to divide by one.

3. Allow system to acquire bit sync and observe phase error at input to DC meter. Adjust phase shift for coincidence of square waves, i.e., zero DC output from mod-2 adder. (The meter is assumed to be calibrated in phase shift at the clock frequency.)

4. On a dual trace scope observe both inputs to the AND gate leading to Error Counter. Verify that the Strobe occurs when the adder output indicates coincidence of both data lines. If not, advance or retard strobe generator without changing phase adjust (step 3).

5. Conduct experiments by recording Mean Absolute Phase Error and Bit Error Count (see Appendix A for guidelines as to length of data run for specified confidence limits on bit error rate).

Conditions that can be varied for these experiments include

a) Signal level

b) Additive noise power

c) Bit transition density (variable divider setting)

d) Clock time base modulation (sinewave amplitude and frequency)

Acquisition time of the bit sync PLL can be measured by periodically interrupting the clock input to the system under test and observing the phase error decay at point A when the clock is re-applied at point B. A scope display synchronized to the switch closure will permit determination of the elapsed time until the phase error remains within a specified tolerance.

7. PCM FRAME SYNC PERFORMANCE EVALUATION

7.1 Introduction

PCM data for telemetry or other applications is generally blocked into frames consisting of large numbers of bits. The frame transition points are identified by frame code bits which provide the mechanism for frame synchronization. The frame bits may be further subdivided into words or channels but these are usually not identified and synchronized by separately allocated bits. Instead word sync is maintained by counting elapsed bits relative to frame transitions.

In order to perform tests on frame synchronization, it is necessary to provide a decoder for the frame codeword. This is most directly accomplished by employing the actual frame decommutator which extracts the individual channels in a time division multiplexed PCM format. The decoder/decommutator will contain a more or less elaborate frame synchronization procedure whose performance must be evaluated in the presence of perturbations due to other system elements. The frame decommutator interfaces with the remainder of the system through the data and clock terminals from the bit synchronizer. Hence the sources of malfunction in frame sync are bit errors and bit slippages.

A bit slippage is a loss or gain in bit count during a frame. This phenomenon can be caused by cycle skipping in the bit sync PLL. Due to bit errors and/or bit slippages the frame sync decoder may fail to identify or erroneously identify frame transitions. In either case, one or more frames will be lost until frame sync is reacquired. Initial acquisition and reacquisition after sync loss proceeds under the control of the frame search and acquisition logic. The design of this logic and the selection of the frame codewords is discussed in the literature. The experiments outlined below could be employed to evaluate performance for various choices of parameters for frame sync logic.

7.2 Principles of Tester

The test configuration described below is intended for tests with real-time decoder decommutators and accessible transmitters. Section 7.4 describes similar experiments for non-accessible transmitters.

The test setup for frame sync evaluation is shown in Fig. 21. For completeness, the simultaneous measurement of bit and clock errors is also shown. A Test Frame Generator (TFG) now takes the place of the previously used Pseudo-Random Sequence Generator. The TFG has capability of

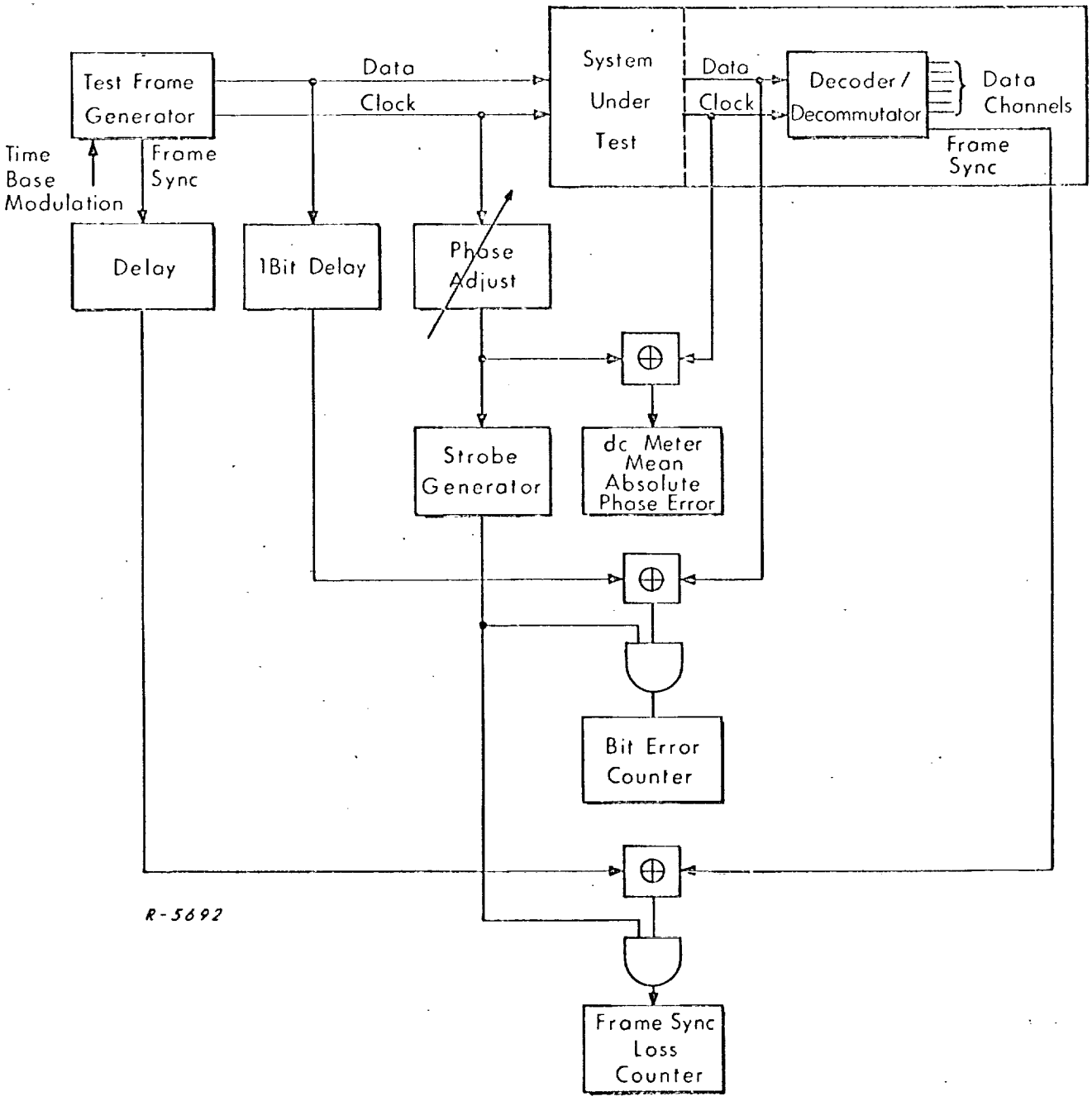

Fig. 21 Frame, Bit and Clock Error Measurements with Accessible Transmitter

simulating a standard PCM frame of moderate length. Within this limit, the TFG can produce an arbitrary bit sequence consisting of a specific framing code plus simulated data bits. The data bits allow the inclusion of various transition densities to test the bit sync extraction as in Sec. 6 .

There are delays required in both the data lines and the frame sync line to compensate for processing delays through the system under test. However, in view of the different method here used for generating variable data transition densities, it becomes possible to include the 1-bit data delay and the frame sync delay within the TFG. The method of incorporating the delays will depend on the detailed design of the TFG which will not be treated here.

The remainder of the test configuration can be understood with reference to the discussion in Sec. 6 . The procedure is essentially the same as before with the addition of one more measurement: the Frame Sync Loss count. The two frame sync lines carry binary logic levels with, say, "1" representing the frame transition clock interval and "0" the remaining frame period. The mod-2 sum of the two lines is strobed into the counter in a manner equivalent to the bit error counter. Note, however, that a frame sync loss adds 2 counts for each frame transition since the "1" output from both lines will produce an increment to the counter. Thus the counter contents must be divided by two to yield the true frame sync loss count.

Frame acquisition time is measured by setting the counter to zero at the start of an experiment. After acquisition the counter will contain (twice) the number of frames elapsed during acquisition. For this test to be valid the counter should be read directly after initial acquisition and before any subsequent frame sync losses have occurred.

7.3 Procedure for Measuring Frame Sync Loss

This procedure requires a Test Frame Generator or Transmitter Simulator corresponding to the PCM decoder/decommutator under test. The details of such a device are not included here since they depend strongly on the specific system characteristics. In other respects the procedure is similar to the one outlined in Sec. 6.3.

1. Assemble test configuration shown in Fig. 21 and connect Data, Clock and Frame Sync inputs and outputs to the system under test.

2. Set clock at data rate to be tested. Set signal level at a nominal value, and remove all external additive noise and time base modulation. Set transition density at maximum.

3. Allow system to acquire bit sync and observe phase error at input to DC meter. Adjust phase shift for coincidence of square waves, i.e., zero DC output from mod-2 adder. (The meter is assumed to be calibrated in phase shift at the clock frequency.)

4. On a dual trace scope observe both inputs to the AND gate leading to Bit Error Counter. Verify that the Strobe occurs when the adder output indicates coincidence of both data lines. If not, advance or retard strobe generator without changing phase adjust (step 3).

5. On a dual trace scope observe both inputs to the AND gate leading to the Frame Sync Loss Counter. Verify that the Strobe occurs when the adder output indicates coincidence of both sync pulses. If not, adjust delay compensation for Frame Sync from Test Frame Generator.

6. Conduct experiments by recording Mean Absolute Phase Error, Bit Error Count and Frame Sync Loss Count (see Appendix A for guidelines as to length of data run for specified confidence limits on bit error rate).

Conditions that can be varied for these experiments include

a) Signal level

b) Additive noise power

c) Bit transition density

d) Clock time base modulation (sinewave amplitude and frequency)

e) Frame sync code sequence

f) Frame synchronization procedure (acquisition and retention strategy)

7.4 Tests with Inaccessible Transmitters

Situations will arise where a system must be tested without access to the transmitter except through the transmission medium itself. Two examples can be cited: when a tape recorder intervenes between signal generation and detection and when a system is tested end-to-end from a remote terminal. In either case, the transmitted data must be synchronously regenerated at the receiving terminal to permit evaluation of performance in terms of Bit Error Rate and Frame Sync Loss. Without access to the transmitter, the regeneration process depends on the clock output from the receiver, and therefore clock phase error relative to the transmitter clock cannot be measured.

The resynthesis of data is accomplished via a duplicate of the transmitter Test Frame Generator or Pseudo Noise Generator. Of particular interest is the evaluation of frame sync performance under conditions of inaccessible transmitters. Since there is no "true" frame sync available for comparison, one must derive from the received data stream an indication of frame sync which is more reliable than the frame sync extraction under test. This objective can be accomplished by making the simulated data periodic at the frame rate and using the total bits in the frame for frame sync test. A loss of frame sync will result in an abnormally high error rate during each misframed block, hence the error count per frame can be used as an indication of frame sync loss.

Figure 22 shows the test configuration for performing error rate and frame sync loss measurements with inaccessible transmitters. The TFG is driven by an external clock and an external frame sync; it produces the framing codeword and a pseudorandom data sequence that repeats each frame. At the receivers, the clock and frame sync are derived from the bit synchronizer and decommutators, respectively. The data from the TFG is compared to the received data and strobed into two counters. The Bit Error Counter plays the same role as in the previous experiments. The upper counter also accumulates bit errors but is reset once per frame.. If the contents of this counter reach a specified threshold level, the overflow indication is passed on to the frame sync loss counter. The overflow point (i.e., threshold) is set to correspond to about 20% or 25% of the frame length in bits. An error rate of this magnitude will not occur in normal operation and is almost certain to arise from loss of frame sync. To prevent multiple overflows during one frame the latching arrangement shown in the figure is provided.

Until loss of frame sync is detected and reacquisition completed by the built-in logic of the decommutator, the counter overflow will reoccur for each missed frame. Hence the contents in the frame sync counter can be

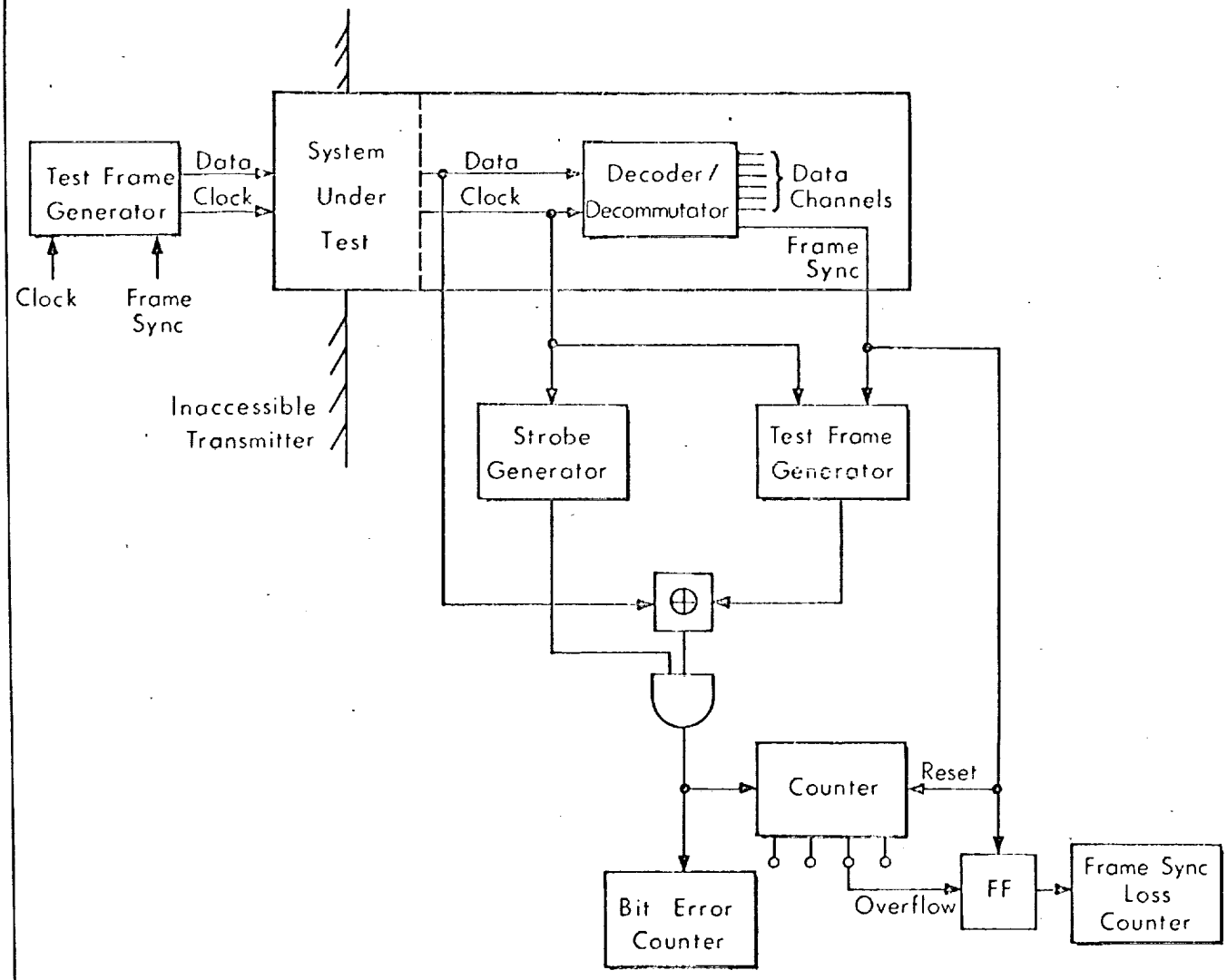

Fig. 22 Bit Error and Frame Sync Loss Measurement with Inaccessible Transmitter

used for measuring initial acquisition or reacquisition time. The errors during lost frames are, of course, also accumulated in the bit error counter. Since these are errors that a real PCM system must contend with, it is appropriate to include them in the bit error rate. The procedures for running experiments with the configuration of Fig. 22 are similar to Secs. 6.3 and 7.3 and will not be repeated here.

Finally we observe that for non-real time evaluation the tests outlined in this subsection can be performed on a digital computer. The frame sync decoder and decommutator, as well as the test frame generation, are simulated in the computer. The received data stream is read into the computer and the bit and frame error counts are derived as above.

REFERENCES

1. 59 IRE 20.S1 Committee, "IRE Standards on Methods of Measuring Noise in Linear Twoparts, 1959," Proc, IRE 48, January 1960, pp. 60 ff.

2. Davenport, W.B., Jr. and W.L. Root, "Random Signals and Noise," Mc-Graw-Hill, p. 207.

3. Vigneri, R., G.G. Gulbenkian, and N. Diepeveen,"A Graphical Method for the Determination of Equivalent Noise Bandwidth," The Microwave Journal, June 1968.

4. Ghais, A.F., E.J. Ferrari, and C.J. Boardman, "Study of Telemetry Receiver and Recorder Phase Linearity Problems," Final Report on Contract AF 19(628)5655 for Air Force Systems Command, Document No. ESD-TR-66-409. Prepared by ADCOM, Inc., August 1966.

5. Telemetry Standards prepared by the Telemetry Working Group of the Inter-Range Instrumentation Group of the Range Commanders' Conference; IRIG Document No. 106-60 (Revised June 1962).

54

[redacted]